Earth-Science Reviews 207 (2020) 103219

Contents lists available at ScienceDirect

Earth-Science Reviews

journal homepage: www.elsevier.com/locate/earscirev

Tectonic significance of Australian rare earth element deposits

Carl Spandler[a,b,*], Paul Slezak[a,c], Teimoor Nazari-Dehkordi[a,d]

[a] Geosciences, James Cook University, Townsville, QLD 4811, Australia
[b] Department of Earth Sciences, The University of Adelaide, SA 5005, Australia
[c] School of Earth Science/iCRAG, University College Dublin, Dublin 4, Ireland
[d] Department of Geology, University of Johannesburg, Johannesburg, South Africa

ARTICLE INFO

Keywords:
Rare earth elements
Ore deposit
Tectonics
Mesoproterozoic
Carbonatite
Australia
Unconformity
Peralkaline

ABSTRACT

Australia is host to a diverse range of rare earth element (REE) ore deposits, and therefore is well placed to be a major supplier of REE into the future. This paper presents a review of the geology and tectonic setting of Australia's hard-rock REE resources. The deposits can be classified into four groups: 1. Carbonatite associated; 2. Peralkaline/alkaline volcanic associated; 3. Unconformity related, and; 4. Skarns and iron-oxide-copper-gold (IOCG) related. With the exception of the unconformity related deposits, all of these deposit groups are directly or indirectly related to continental alkaline magmatism. Extensive fractional crystallisation and/or igneous accumulation of REE minerals were essential ore-forming processes for carbonatite-associated and peralkaline/alkaline volcanic-associated deposits, while hydrothermal transport and concentration of REE sourced from basement rocks was responsible for producing ore in unconformity-related, skarns and, potentially, IOCG deposits. The economic potential of many deposits has also been enhanced by supergene alteration processes.

All of Australia's REE deposits formed in an intracontinental setting in association with crustal-scale fault zones or structures that acted as transport conduits for ore-forming magmas or fluids. Most deposits formed in the Mesoproterozoic under conditions of relative tectonic quiescence. There is little evidence for the involvement of mantle plumes, with the exception of the Cenozoic peralkaline volcanic systems of eastern Australia, and possibly the IOCG deposits. Instead, ore productive magmas were generated by melting of previously-enriched mantle lithosphere in response to disruption of the lithosphere-asthenophere boundary due to fault activation. REE minerals in many deposits also record episodes of recrystallisation/resetting due to far-field effects of orogenic activity that may significantly postdate primary ore formation. Therefore, REE orebodies can be effective recorders of intracontinental deformation events.

In general, Australia's inventory of REE deposits is similar to the global record. Globally, the Mesoproterozoic appears to be a particularly productive time period for forming REE orebodies due to favourable conditions for generating ore-fertile magmas and favourable preservation potential due to a general lack of aggressive continental recycling (i.e., active plate tectonics).

1. Introduction

The recent rise of rare earth elements (REE) as essential metals for modern technology has spurred global efforts to discover new REE orebodies. These orebodies are now recognised from a variety of geological settings across the globe (Weng et al., 2013, 2015; Van Gosen et al., 2017), but very few are currently being mined to produce REE. Presently, most of the world's REE are sourced from China, although Australia is emerging as a major alternative supplier, with two operations (Mount Weld and Browns Range) in production and several advanced projects that are projected to supply REE products in the near future.

Australia's REE resources include a diverse range of ore deposit types, among which the primary hard-rock deposits tend to have the highest grades and tonnages (Fig. 1), and generally are considered to be of most economic significance (Jaireth et al., 2014). Although descriptions of Australia's major REE resources have been presented by Hoatson et al. (2011) and Jaireth et al. (2014), there has since been substantial additional resource definition and exploration work, and significant progress has been made in understanding the age, geological setting and evolution of many deposits. In particular, recent studies have utilised the geochronological and geochemical/isotopic archive of REE ore minerals, such as monazite, xenotime and apatite, to resolve metal sources and the temporal and geodynamic setting of ore

* Corresponding author at: Department of Earth Sciences, The University of Adelaide, SA 5005, Australia.
E-mail address: carl.spandler@adelaide.edu.au (C. Spandler).

https://doi.org/10.1016/j.earscirev.2020.103219
Received 12 February 2020; Received in revised form 21 May 2020; Accepted 26 May 2020
Available online 05 June 2020
0012-8252/

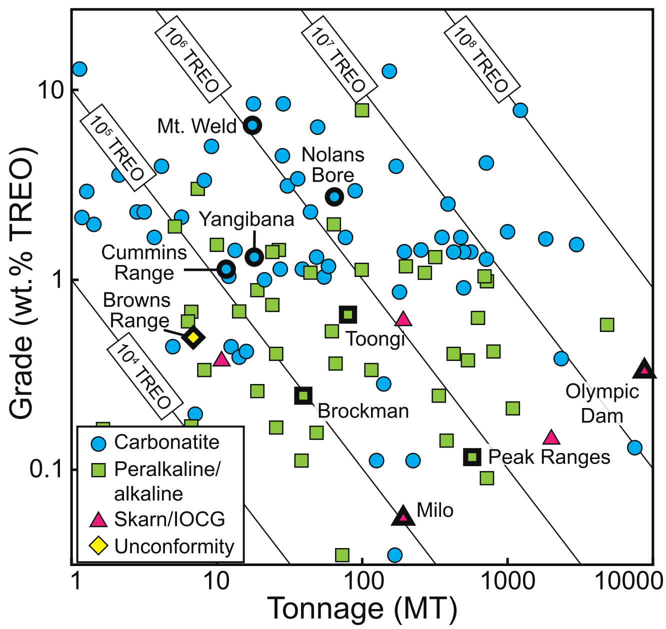

Fig. 1. Grade versus tonnage of Australian hard-rock REE deposits (bold symbols with deposit names) compared to global REE deposits (modified after Weng et al., 2015).

formation (e.g., Downes et al., 2016; Huston et al., 2016; Spandler and Morris, 2016; Nazari-Dehkordi et al., 2018, 2020). These ore minerals are often susceptible to hydrothermal or tectonic resetting/recrystallisation, and so may also record geological activity that postdates primary ore formation (e.g., Schoneveld et al., 2015; Anenburg et al., 2018; Slezak and Spandler, 2019).

In this paper we provide an overview of the geology of Australia's hard-rock REE ore deposits. The economic viability of mining these deposits is controlled not only by ore grade and tonnage, but also by aspects of ore mineralogy, environmental issues (including treatment of radionuclides), and costs of transportation, infrastructure and ore processing (see Weng et al., 2015). These aspects of the economics of mineral extraction are not dealt with in this paper; instead, here we focus on the geological evolution of the deposits, with emphasis placed on their tectonic setting of formation, and their modification due to subsequent tectonic/hydrothermal activity. We demonstrate that REE ore deposits can be effective records of tectonic events, including, in some cases, far-field tectonic activity that is not well preserved in the immediately surrounding rock units. We also examine commonalities between the Australian and global records of REE mineralisation, from which we surmise that REE orebodies may also be useful for understanding the geological evolution of continental interiors over long periods of Earth history.

2. REE ore deposits of Australia

Australia's REE ore deposits are located across the continent (Figs. 2, 3), and collectively span an age range from the Paleoproterozoic to Tertiary (Jaireth et al., 2014). Mineralisation styles include monazite sand deposits (placers), laterites, pegmatites, sedimentary phosphorite deposits, carbonatite-related, peralkaline/alkaline volcanic-related, unconformity-related, skarns and iron-oxide copper-gold (IOCG) deposits (Jaireth et al., 2014; Mudd and Jowitt, 2016; Nazari-Dehkordi et al., 2018). This diversity of mineral deposit types is testament to Australia's protracted and diverse geological evolution, and provides optimism that further REE resources remain to be discovered in the near future. Geological characteristics of the principal hard-rock deposit styles are described below and summarised in Table 1. Here, we examine ore types under four groups; carbonatite associated; peralkaline/alkaline volcanic associated; unconformity related, and; skarns and IOCG related (Figs. 1, 2).

2.1. *Carbonatite associated*

Records of carbonatite magmatism are relatively rare on the Australian continent, but nonetheless, these rocks are among the most prospective for REE resources. Most Australian carbonatites were emplaced in the Meso- to Neoproterozoic, into Proterozoic mobile belts (Downes et al., 2016), and subsequently reached economic REE grades due to secondary REE enrichment by lateritic alteration of carbonatite parent rock. Significant carbonatite-related REE ore deposits/districts include Yangibana, Cummins Range, Mount Weld, and Nolans Bore.

2.1.1. *Yangibana*

Yangibana is a light REE ore district directly associated with the Gifford Creek Carbonatite Complex in the Gascoyne region of Western Australia (Pearson et al., 1996; Pirajno et al., 2014; Slezak and Spandler, 2019, 2020). Most of the orebodies are dyke-like “ironstones”, which may be several metres wide and hundreds of metres in strike length. The orebodies are distributed over an area of ~180 km^2, and collectively represent a JORC resource of 21.7 million tonnes (Mt.) of ore at 1.17% total REE oxides (TREO) (Hastings Technology Metals Limited, 2019), Monazite and subordinate rhabdophane are the ore minerals, with Nd and Pr being the target metals of economic interest.

The Gifford Creek Carbonatite Complex is exposed as series of discrete alkaline/carbonatitic dyke/sill swarms that extend over distances of between 1 and 15 km (see Slezak and Spandler, 2020). The complex intrudes granites and metasedimentary rocks (Durlacher Supersuite and Pooranoo Metamorphics) of the Mesoproterozoic Gascoyne Province, which represents the conjoining orogenic zone between the Archaean Yilgarn Craton, Glenburgh Terrane and Pilbara Craton (see Johnson et al., 2013 for more details). Rock types of the complex include calcite to dolomite carbonatites (Lyons River Sills), ferrocarbonatites, magnetite-biotite dykes, fenites, and alkali-rich magmatic-hydrothermal veins/dykes (Slezak et al., 2018; Slezak and Spandler, 2020). The major structures in the area are the NW-SE trending Lyons River Fault that bounds the complex to the south and west, and the Bald Hill Lineament that transects the northeastern portion of the Complex and trends subparallel to the Lyons River Fault (Slezak and Spandler, 2019, 2020). The Lyons River Fault is recognised to be a lithospheric-scale structure that represents the suture between the Neoarchean Glenburgh Terrane and the Pilbara Craton (Johnson et al., 2013).

The Gifford Creek Carbonatite Complex was emplaced at 1370 Ma (Zi et al., 2017; Slezak and Spandler, 2019); a time that does not correspond to any major magmatic or tectonic activity in Australia. Our preferred hypothesis is that carbonatite magmatism was generated by low degree melting of a mantle source that was fertilised by subduction processes during convergence between the Yilgarn and Glenburgh Terrane at ca. 2.0 Ga (Slezak and Spandler, 2020). Mantle melting was likely triggered by reactivation of the Lyons River Fault in response to far-field stresses associated with the initial rifting of the North China Craton from the Western Australian Craton (Slezak and Spandler, 2019; Fig. 4). The Lyons River Fault also acted as a conduit for magma transfer to the upper crust. Ore grade mineralisation at Yangibana was reached by a combination of REE enrichment via crystal fractionation of ferrocarbonatites, followed by sustained supergene enrichment to produce the REE-rich ironstones (Pirajno et al., 2014; Slezak, 2019).

Rocks of the complex record multiple episodes of hydrothermal and/or tectonic activity that occurred subsequent to igneous emplacement. Uranium–Th–Pb and Sm–Nd isotope systems of apatite and monazite record the effects of regional orogenic/tectonic activity including the 1320–1170 Ma Mutherbukin Tectonic Event, the 1080–950 Ma Giles Event and Edmundian Orogeny, and the 955–820 Ma Kuparr Tectonic Event (Slezak and Spandler, 2019; Olierook et al., 2019; Fig. 5). The isotopic signatures recording these

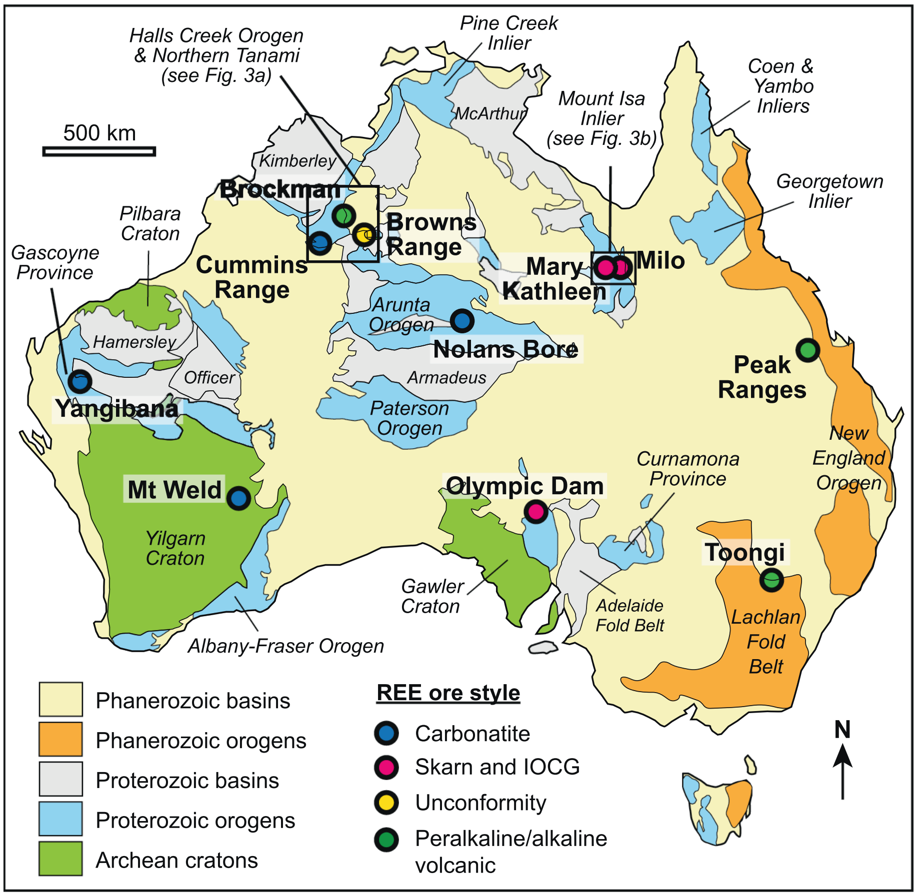

Fig. 2. Geological architecture of Australia with locations of hard-rock REE ore deposits.

events reflect internal resetting and recrystallisation of existing ore minerals, rather than input of external sources such as mantle-derived melts (Fig. 6a).

2.1.2. Cummins Range

The Cummins Range Carbonatite Complex is located at the southern margin of the Kimberley Craton, Western Australia, close to the junction between the Paleoproterozoic Halls Creek Orogen and King Leopold orogenic belt (Figs. 2, 3a). The complex also lies in close proximity to the regional scale NNE-trending Hall Creek Fault (Fig. 3a; Downes et al., 2014, 2016). The complex is a ~ 1.5 km wide composite, near-vertical stock of variably metasomatised phlogopite-diopside clinopyroxenite cored by a plug of calcite and dolomite carbonatite dykes (Downes et al., 2014). These rock units intrude Paleoproterozoic metasedimentary rocks of the Lamboo Province and, in turn, are cut by steep NNW trending shear zones that include strongly-foliated carbonatites, phlogopitite and apatite-monazite (± talc, amphibole) rock that contains ore grade (i.e., wt% levels) REE contents (Downes et al., 2014). The main ore minerals are monazite and apatite, with minor amounts of REE-fluorocarbonate minerals. At the time of writing, a maiden JORC resource of 13 Mt. of ore grading at 1.13% TREO has been delineated in the deeply weathered cap to the intrusive complex (RareX Ltd., 2020).

The alkaline complex is interpreted to have formed at ~1.0 Ga (Downes et al., 2016) via partial melting of an enriched mantle source that was previously metasomatised by Paleoproterozoic plate subduction either along the southern margin of the Kimberley Craton (Downes et al., 2014), or alternatively along the eastern margin of the Craton prior to, and during, development of the Halls Creek Orogeny (Kohanpour et al., 2017). The diversity of rock types of the complex is in part ascribed to magma differentiation and cumulate processes, although some degree of crustal contamination of the magmas is inferred based on stable isotope data (Downes et al., 2014). The primary REE mineralisation, including the apatite-monazite rock, is interpreted to be at least partly of hydrothermal origin (Downes et al., 2014), with the hydrothermal activity most probably linked to igneous emplacement of the complex.

Formation of the complex at ~1.0 Ga is not related to any regional scale magmatism such as a large igneous province. Instead, igneous emplacement is suggested to result from low-degree melt extraction from the mantle due to reactivation of lithospheric scale structures within the Halls Creek Orogen in response to continental-scale plate reorganisation (Downes et al., 2016). As with Yangibana, U-Th-Pb dating of monazite from Cummins Range records isotopic resetting events related to younger orogenic activity; in this case, the Yampi and King Leopold Orogenies at ~900 Ma and ~ 590 Ma, respectively (Downes et al., 2016; Fig. 5).

2.1.3. Mount Weld

Mount Weld, located 35 kms southeast of Laverton in Western Australia, represents one of the highest-grade REE deposits in the world (Fig. 1), with 23.2 Mt. of ore grading at 7.5% TREO, as well as economically significant levels of Nb, Ta and P_2O_5 (Lynas Corp. Ltd., 2015). The mineral resource is hosted in a diverse suite of ore minerals (mainly monazite, churchite, plumbogummite-group minerals, and rhabdophane; Lottermoser, 1990) within a supergene laterite zone, up to 90 m thick, that overlies a ~ 4 km diameter, steeply-plunging cylindrical carbonatite intrusion (Willett et al., 1986; Lottermoser, 1990), or diatreme (Pirajno, 2015). The carbonatite was emplaced into late Archean volcano-sedimentary sequences in the Laverton Tectonic Zone, which is a lithospheric-scale deformation zone that marks the boundary between the Kurnalpi and Burtville Terranes of the Yilgarn Craton

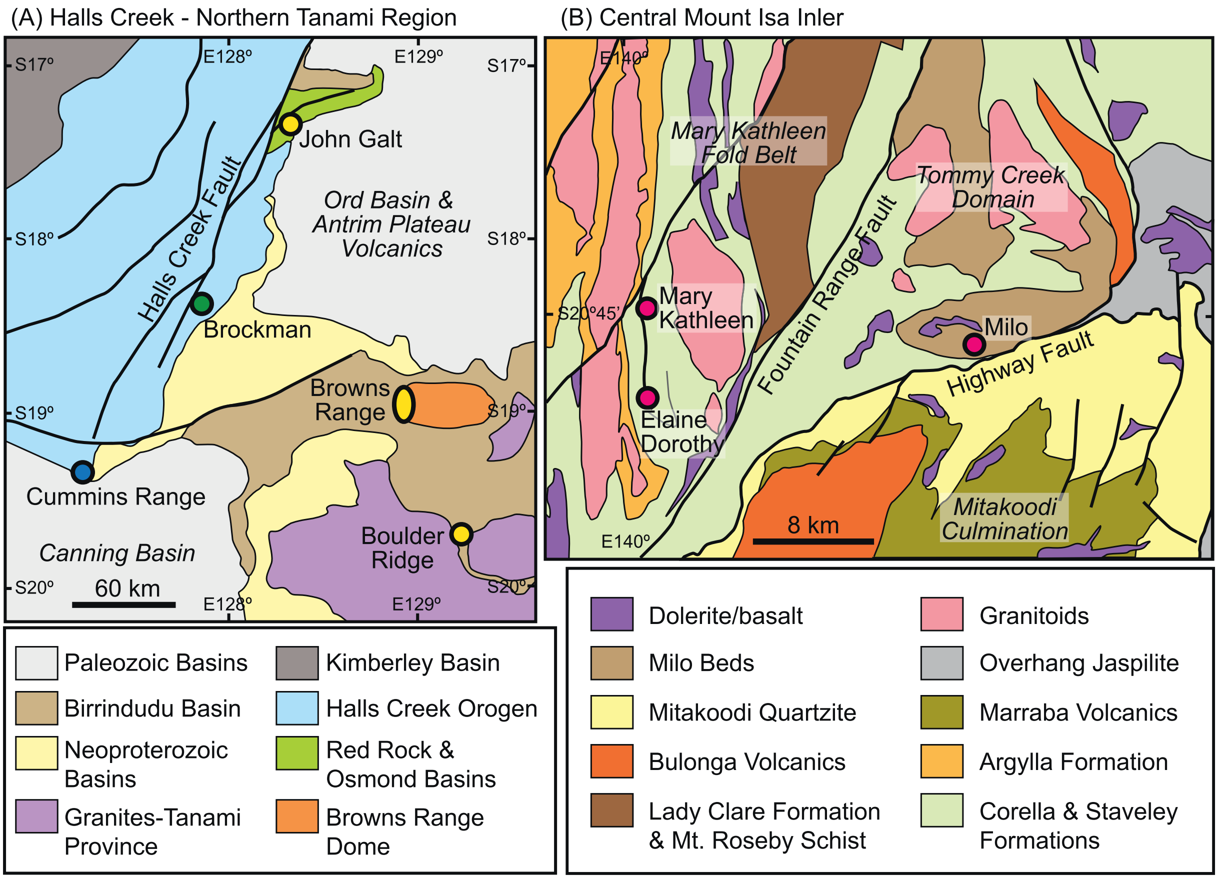

Fig. 3. Regional scale geological maps of; (A) the Halls Creek- Northern Tanami District and; (B) the central Mount Isa Inlier, showing the location of REE deposits and associated major structural elements. See Fig. 2 for map locations.

(Henson et al., 2010). The trigger for magma production at this time is poorly understood.

The primary carbonatite complex consists largely of coarse calcite carbonatite, with minor dolomite carbonatite, ferrocarbonatite and phoscorite. These rocks are enveloped by a 0.5 km wide glimmerite alteration zone. Cumulate textures, layering and flow banding have been observed in drillcore (Willett et al., 1986). Stable and radiogenic isotope analysis indicates that the carbonatite complex was emplaced at ~2025 Ma, and that the magma was derived from melting of a mantle source that was likely enriched by metasomatic components in a convergent margin setting between 2710 and 2650 Ma (Nelson et al., 1988; Graham et al., 2004; Czarnota et al., 2010). The Laverton Tectonic Zone likely acted as a conduit to allow magma emplacement into the upper crust. Sustained supergene weathering of the carbonatite during the Mesozoic and Cenozoic led to decomposition of primary carbonate minerals to produce an apatite-rich residuum zone blanketed by a supergene zone with secondary REE ore minerals (Lottermoser, 1990).

2.1.4. Nolans Bore

Nolans Bore is located in the Reynolds Range of the Aileron Province, Central Australia (Fig. 2). The region has a complex geological history with major orogenic/deformation episodes at around 1.8 Ga (the Stafford Event), 1.78 Ga (Yamba Event), ~1.7 Ga (Strangway Orogeny), 1.6 to 1.52 Ga (Chewings Orogeny), 1.5 to 1.4 Ga (Redbank shear zone), and finally the 450 to 300 Ma Alice Spring Orogeny (Schoneveld et al., 2015).

Nolans Bore, held by Arafura Resources Ltd., is a stockwork vein-style light REE deposit containing a 56 Mt. mineral resource grading at 2.6% TREO (Fig. 1; Huston et al., 2016). Fluorapatite is the main ore mineral, although weathering of these ores has produced a high-grade, cheralite-bearing kaolinitic horizon across all zones. The host rocks to the deposit are the granulite–grade Boothby Orthogneiss and Landers Group metasediments. The identified mineral resource covers an area of 1.5 km by 1.2 km, and extends from the surface down to at depth of at least 220 m, with mineralisation open at depth.

The deposit comprises three zones: the north zone, the central zone and southeast zone. The bulk of the REE mineralisation in the north and southeast zones is contained within steeply dipping, NE trending fluorapatite veins with 4–6 wt% REE. These veins are enveloped by relatively thin (< 1 m) clinopyroxene + amphibole (± garnet, ± K-feldspar, ± quartz, ± calcite) alteration selvages (Huston et al., 2016; Anenburg et al., 2020). The central zone consists of N-S trending ore lenses, comprising highly sheared and brecciated apatite-allanite-epidote ore with a broad quartz + epidote ± amphibole alteration envelope (Schoneveld et al., 2015).

The timing of primary ore formation has been constrained to between 1.55 and 1.52 Ga (Huston et al., 2016); this age is similar to the age of pegmatites of the Boothy Orthogneiss, and marks the termination of the Chewing Orogeny. Huston et al. (2016) suggest that the primary mineralisation formed from halogen- and phosphate-rich alkali fluids that evolved from mantle-derived alkaline magmatism, whereas Anenburg and Mavrogenes (2018) and Anenburg et al. (2020) provide a compelling case that Nolans Bore may be the product of reaction between carbonatite magma and silicate wall rocks (so-called ‘antiskarn’) at mid to lower crustal levels. In either case, the parental magma for the mineralisation or mineralising fluids were likely generated by low-degree melting of the lithospheric mantle that was previously enriched by convergent margin tectonics during the Stafford and Strangway Orogenies (Huston et al., 2016).

Isotopic analysis of ore samples show that there has been multiple

Table 1
Geological characteristics of Australia's hard-rock REE ore deposits.

Deposit	Deposit type	REE ore minerals	Mineralisation age (Ma)	Initial εNd	Tectonic setting	Pre-mineralisation lithosphere fertilisation event	Associated crustal-scale fault/lineament	Post-mineralisation reworking/resetting age (Ma)	References
Yangibana	carbonatite (LREE)	monazite, rhabdophane (sb)	1370	−2 to −4.5	intra-continental	2.0 Ga Glenburgh Orogeny	Lyons River Fault	ca. 1320–1170, 1080–950, 955–820	1, 2, 3
Cummins Range	carbonatite (LREE)	apatite, monazite REE-carbonates (sb)	ca. 1000	+1.6 to +2.4	intra-continental	1.9 to 1.8 Ga Halls Creek Orogeny	Halls Creek Fault, Willowra Lineament	ca. 900, 590	4
Mount Weld	carbonatite (LREE)	monazite, churchite, rhabdophane, REE-Al phosphates[a], apatite (sb), cerianite (sb)	2025	~ +0.5	intra-continental	2.71 to 2.65 Ga, Yilgarn Craton	Laverton Tectonic Zone		5, 6, 7
Nolans Bore	carbonatite (LREE)	apatite, cheralite, allanite, REE-Al phosphates[a], monazite (sb)	ca. 1530	~ −4	intra-continental	1.8 to 1.7 Ga Stafford & Strangways Events	Aileron Shear Zone	ca. 1400, ca. 900, 450–300	8, 9, 10
Toongi	peralkaline volcanic (HREE, Zr, Hf, Nb, Ta)	REE-carbonates, Zr alkali silicates, Y-milarite (sb)	ca. 185	+3 to +4	intra-continental	> 500 to ca. 350 Ma, Lachlan Fold Belt	Lachlan Fold Belt – Gunnedah Basin boundary	–	11
Brockman	alkaline volcanic (HREE, Nb)	Zr silicates, thorite, REE-niobates, REE-carbonates	1850	~ +2	continental rift	ca. 2.7 Ga, ca. 2.5 Ga North Australian Craton	Halls Creek Fault	–	12, 13, 14
Peak Ranges	peralkaline volcanic (HREE, Zr)	Zr alkali silicates, REE-carbonates, REE-silicate (sb)	29	+2.8 to +3.3	hot spot/mantle plume	> 500 to ca. 240 Ma Thomson and New England Orogens	Thomson Orogen – New England Orogen boundary	–	15
Browns Range	unconformity –related (HREE)	xenotime, florencite	1650–1620	−14 to −25	intra-continental	–	–	1600 to 1500	16
Mary Kathleen - Elaine	skarn (LREE)	allanite, uraninite, stillwellite	1520	~ −9	orogenic?	1.74 Ga Wonga Event ca. 1.6 Ga Isan Orogeny	Mary Kathleen Shear Zone	1510	17,18
Milo	IOCG (LREE)	apatite, allanite (sb), titanite (sb), REE-carbonates (sb)	ca. 1600 to 1500	~ −5	orogenic?	1.74 Ga Wonga Event? ca. 1.6 Ga Isan Orogeny?	Highway Fault Zone	ca. 1550	19, 20
Olympic Dam	IOCG (LREE)	REE-carbonates, florencite, xenotime, monazite (sb)	1590	−2.5	intra-continental extension	ca. 2.5 Ga, Gawler Craton 1.73–1.69 Kimblan Orogeny	Intersection of NNW & WNW trending lineaments	1400–1370, ca. 1100, 820, 450–300, 200?	21, 22, 23, 24

References: 1= Pearson et al. (1996), 2 = Slezak and Spandler (2019, 2020), 3 = Zi et al. (2017), 4 = Downes et al. (2014, 2016), 5 = Willett et al. (1986), 6 = Lottermoser (1990), 7 = Graham et al. (2004), 8 = Schoneveld et al. (2015), 9 = Huston et al. (2016), 10 = Anenburg and Mavrogenes (2018), 11 = Spandler and Morris (2016), 12 = Ramsden et al. (1993), 13 = Taylor et al. (1995a, 1995b), 14 = Blake et al. (1999), 15 = Chandler and Spandler (2020), 16 = Nazari-Dehkordi et al. (2017, 2018, 2019, 2020), 17 = Oliver et al. (1999), 18 = Spandler et al. (2016), 19 = Harvey (2014), 20 = this study, 21 = Ehrig et al. (2012), 22 = Schmandt et al. (2017, 2019), 23 = Cherry et al. (2018), 24 = Hall et al. (2018)

(sb) = subordinate.

[a] REE-Al phosphates include Plumbogummite-group minerals.

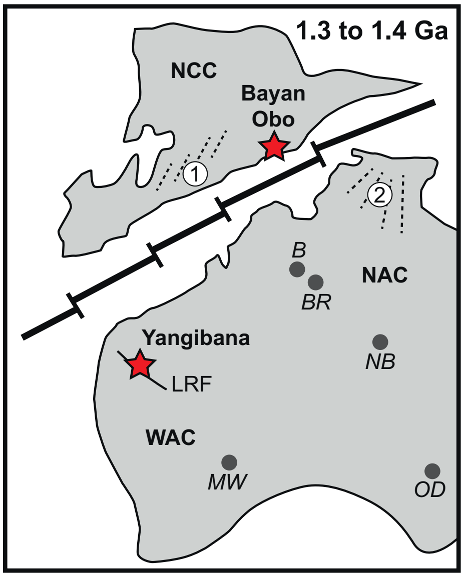

Fig. 4. Paleogeographic reconstruction of the North Australia Craton (NAC), West Australia Craton (WAC) and North China Craton (NNC) from 1.3 to 1.4 Ga (modified after Pisarevsky et al., 2003). Dykes/sills swarms emplaced during this period include; (1) 1.33 to 1.30 Ga Yanliao and; (2) ca. 1.33 Ga Derim Derim (Zhang et al., 2017). LRF = Lyons River Fault. Australian REE ore deposits formed at this time; B = Brockman, BR = Browns Range, NB = Nolans Bore, OD = Olympic Dam, MW = Mount Weld. Note, the distal location of Yangibana from the continental rift zone, and location of Bayan Obo on the opposing side of the rift.

episodes of recystallisation and reworking of the ore zones that extend to over 1 billion years after primary formation (Figs. 5, 6). Reworking events have been identified at ca. 1400 Ma (Schoneveld et al., 2015; Huston et al., 2016; Anenburg et al., 2020), which may be related to deformation associated with the Redbank Shear Zone, and between 450 and 300 Ma (Fig. 5). This latter episode corresponds to the Alice Springs Orogeny, and was responsible for formation of most of the brecciation and hydrothermal alteration of the Central Zone (Schoneveld et al., 2015). This event is likely to be related to exhumation of the deposit (Huston et al., 2016), with brecciation and recystallisation driven by infiltration of either magmatic, or mixed metamorphic and meteoric fluids at 450–600 °C (Schoneveld et al., 2015).

2.2. Peralkaline/Alkaline volcanic associated

Globally, peralkaline silicate plutonic complexes host significant REE—particularly heavy REE—mineralisation as well as significant Zr, Nb, Hf, and Ta resources (Weng et al., 2015). Australian examples of this mineralisation style are somewhat unusual as they are directly associated with volcanic, rather than plutonic, systems. Significant ore deposits include Toongi in New South Wales, and Brockman in Western Australia, while Cenozoic alkaline volcanic complexes of eastern Australia represent prospective targets for further mineralisation.

2.2.1. Toongi

The Toongi deposit (also known as the Dubbo Zirconia Project) is located approximately 20 km south of Dubbo in central New South Wales (Fig. 2). The deposit consists of ~73 Mt. of mineral resources (measured and inferred) grading at 1.96 wt% ZrO_2, 0.04 wt% HfO_2, 0.45 wt% Nb_2O_5, 0.03 wt% Ta_2O_5, 0.14 wt% Y_2O_3 and 0.75 wt% TREO (Alkane Resources Ltd., 2015), all of which is contained within a 0.3 km^2 elliptical trachyte laccolith. This mineralised laccolith is one of a number of small (> 2 km^2) trachytic to syenitic plugs, flows and laccoliths that collectively form the Toongi Alkaline Magma Field Spandler and Morris, 2016).

Toongi lies at the boundary between the Permo-Triassic Gunnedah Basin to the north and Late Cambrian to Carboniferous Lachlan Fold

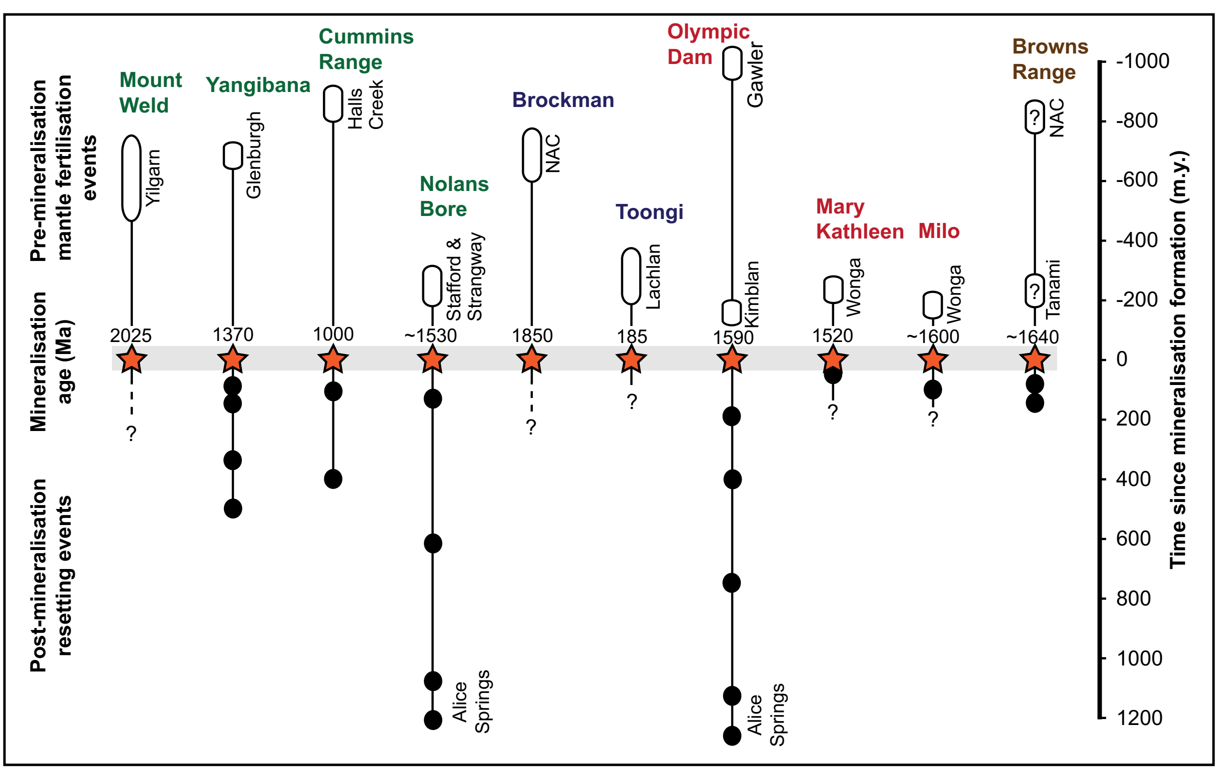

Fig. 5. Temporal record of Australian REE ore deposits. Orogenic/convergent margin events that predate mineralisation formation ages are shown at the top of the diagram (negative ages on right side axis) and post-mineralisation resetting events are towards the bottom of the figure (positive ages on right side axis). Literature references for geochronological data for each deposit are provided in Table 1.

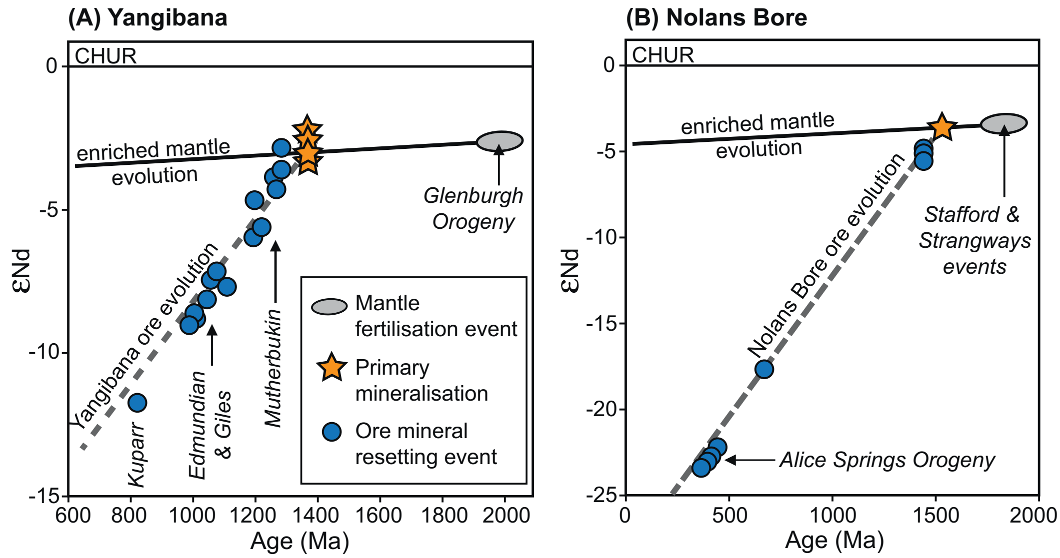

Fig. 6. Neodymium isotope evolution of the (A) Yangibana and (B) Nolans Bore REE deposits. Data for Yangibana are from Slezak and Spandler (2019, 2020) and data for Nolans Bore are from Schoneveld et al. (2015), Huston et al. (2016) and Anenburg et al. (2020). In both cases, isotope data for post-mineralisation resetting events closely follow the modelled isotope evolution trend of REE ores after the time of ore formation (grey dashed trends). This indicates that the resetting events involved closed-system recrystallisation of REE minerals without any additional input of mantle-derived magmatism. The enriched mantle evolution trend was calculated using $^{147}Sm/^{144}Nd$ of model EM2 from Workman et al. (2004), and the ore evolution trend was calculated using $^{147}Sm/^{144}Nd$ of the representative bulk ore in each case. Both isotope evolution models are pinned to the εNd of the ore at the time of primary ore formation.

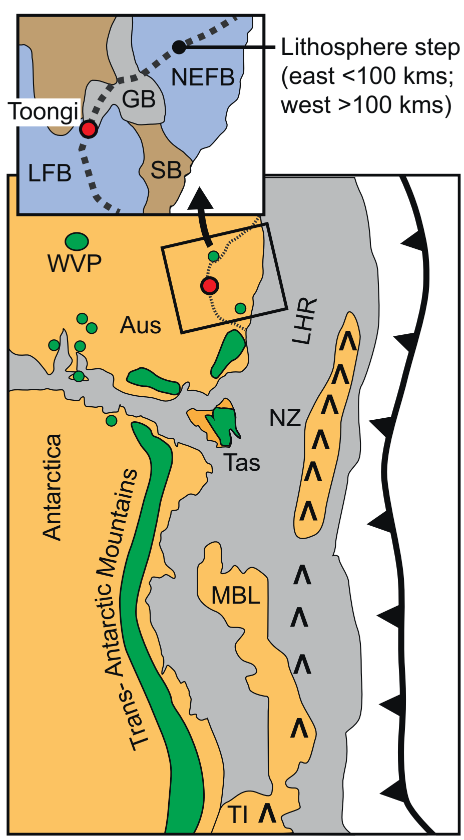

Fig. 7. Early Jurassic paleogeographic reconstruction of eastern Gondwana with magmatic rocks of the Karoo-Ferrar-SE Australia large igneous province shown in green. The Toongi deposit (red dot) is among the most northern expressions of this magmatic event. The deposit lies on the boundary between the Lachlan Fold Belt and Gunnedah Basin and immediately above a distinct step in the lithosphere (adapted from Veevers, 2012, and Davies and Rawlinson, 2014). (For interpretation of the references to colour in this figure legend, the reader is referred to the web version of this article.)

Belt to the south (Fig. 7). The alkaline magmatic bodies were emplaced into, and onto, Siluro-Devonian sedimentary units of the Lachlan Fold Belt and sandstones and siltstones of the Triassic Napperby Formation of the Gunnedah Basin. The Toongi deposit intrusion outcrops at the surface and extends to between ~50 and 150 m in depth. The deposit primarily consists of fine-grained (< 0.5 mm) trachyte with a primary mineralogy dominated by alkali-feldspars (either albite or K-feldspar) and aegirine, although this assemblage has undergone variable degrees of hydrothermal alteration to sericite, ± chlorite ± goethite.

There is a remarkable level of homogeneity in ore grade, and in the mineralogy and textural setting of the ore minerals across the Toongi deposit. Most of the ore metals are contained within a complex Na–Ca–Zr silicate phase, likely REE-rich eudialyte, that mainly occur as sub-spherical to irregular shaped blebs, or "snowballs" that are dispersed throughout the rock matrix (Spandler and Morris, 2016). Niobium and Ta is primarily hosted in lueshite/natroniobite ($NaNbO_3$) that is found as small (< 40 μm) irregular grains that formed in the interstices between igneous matrix grains. REE-rich eudialyte and lueshite/natroniobite are interpreted to be primary magmatic phases. A secondary ore mineral assemblage of Ca–Na–Zr silicates (vlasovite, catapleiite and gaidonnayite) and REE fluoro-carbonates is found infilling vesicles and micro-fractures in the rock. This ore assemblage is associated with sericite and chlorite alteration within the rock matrix, or with quartz and Y-milarite as vesicle-filling phases.

The timing of magmatism has been dated to the early Jurassic (Meakin and Morgan, 1999), which coincides with the emplacement of the Karoo-Ferrar-SE Australia large igneous province that formed during continental extension related to Pangea breakup (Veevers, 2012). Plate reconstructions to this time place the Dubbo region at the northern extent of this magmatic belt (Veevers, 2012), so we suggest that the alkaline magmatism associated with the Toongi Deposit represents a distal expression of the Karoo-Ferrar-SE Australia large igneous province. Toongi also overlies a pronounced step in lithospheric thickness from ca. 100 km in the east, to ca. 140 km in the west, as defined from seismic tomography models (Davies and Rawlinson, 2014; Fig. 7). The timing of formation of this lithospheric step is unknown, but conceivably developed during the Permian extension phase that formed the Surat and/or Gunnedah Basins (Korsch and Totterdell, 2009), and hence would have existed during the late Jurassic. We therefore favour a model for magma generation and focusing by melting of mantle due to edge-driven convection of asthenosphere (e.g., King and Anderson, 1998; Davies and Rawlinson, 2014) along this lithospheric step. This lithospheric step was again a focus of magmatism during the Cenozoic (Zhang and O'Reilly, 1997), possibly due to mantle plume activity, renewed mantle flow or asthenosphere shear (e.g., Conrad et al., 2011).

The boundary between the Lachlan Fold Belt and Gunnedah Basin (Fig. 7) represents a crustal-scale structure that may have allowed mantle-derived magma to traverse the crust towards the surface. The rare metal enrichment to ore grades in the Toongi Deposit trachyte is attributed largely to extreme polybaric fractional crystallisation processes under low H_2O and fO_2 conditions (Spandler and Morris, 2016). A large gravity high that directly underlies the local area is interpreted to represent the remnant mafic/ultramafic differentiates of this fractionation process within the crust (Meakin and Morgan, 1999). A magmatic origin for mineralisation is also consistent with the ore mineralogy and textures, and homogenous distribution throughout the intrusion.

The secondary ore mineral assemblage is interpreted to have formed via post-magmatic hydrothermal alteration by Ca-bearing CO_2–H_2O fluids that were derived either from the crystallising and cooling laccolith, or from localised devolatilisation of the sedimentary country rocks (Spandler and Morris, 2016). Nevertheless, metal redistribution during this alteration was likely limited to the sub metre scale.

2.2.2. Brockman

The Brockman deposit, with a JORC resource of 41.4 Mt. at 0.9% ZrO_2, 0.36% Nb_2O_5, and 0.21% TREO (Hastings Technology Metals Limited, 2019), lies 18 km southeast of Halls Creek in northern Western Australia (Fig. 3a). Despite the relatively low REE grade, the economic value of the deposit is enhanced by a notable enrichment in heavy REE and Nb. The ore is restricted to a single steeply-dipping volcaniclastic unit, known as the Niobium Tuff, that varies from 5 to 35 m in thickness and can be followed along strike for at least 3.5 kms. Mineralisation extends down at least 250 m from the surface, and remains open at depth. The deposit lies in close proximity to the Halls Creek Fault system, which represents a major lithospheric suture zone (Kohanpour et al., 2017).

The Niobium Tuff is the basal unit of the Butchers Gully Member of the Olympio Formation in the Eastern Zone of the Halls Creek Orogen (Blake et al., 1999). The Butchers Gully Member consists of a series of intermediate to felsic alkaline lavas and volcaniclastic rocks that erupted into a rift-related shallow marine environment (Taylor et al., 1995a). The Niobium Tuff is a fine-grained, rhyolitic ash-flow tuff unit with pumice and lithic fragments, and occasional microphenocrysts of quartz and albitised feldspars. The rock mass was subsequently altered by F-bearing fluids to an assemblage of biotite, sericite, chlorite, Fe-rich carbonates and fluorite (Ramsden et al., 1993; Taylor et al., 1995a). The ore metals are hosted by an array of fine-grained secondary minerals including a hydrous 'zircon-gel' phase, thorite, columbite, samarskite and various REE fluorcarbonates (Ramsden et al., 1993). Minor base metal sulfides (primarily sphalerite) and cassiterite are also found in some ore samples.

The Eastern Zone of the Halls Creek Orogen developed between ca. 1910 and 1830 Ma as a mixed clastic sedimentary and alkaline volcanic sequence along the western margin of the North Australia Craton (Tyler et al., 2012). Deposition of the Niobium Tuff has been dated to ca. 1850 Ma (Blake et al., 1999), which corresponds to the timing of transition from a passive margin to active extension and thinning of the continental margin. Geochemical and isotopic data are consistent with a primitive mantle magma source, possibly with some minor contribution for the Paleoproterozoic or late Archean continental basement (Taylor et al., 1995a, 1995b). Ore grade rare metal (e.g., REE, Y, Zr, Nb, Hf, Ta) contents were reached via extensive fractional crystallisation of the alkaline parental magma prior to eruption, with high magmatic F contents likely playing an important role in retaining the ore elements in the fractionating magma (Ramsden et al., 1993; Taylor et al., 1995b). Formation of the Niobium Tuff in a submarine setting (Taylor et al., 1995a) may have prevented significant rare-metal devolatilisation during eruption. Fluorine rich hydrothermal fluids may also have facilitated late-stage remobilisation of ore metals, albeit on a relatively small scale (Taylor et al., 1995b). Finally, the mineralised unit was folded and tilted due to collision of the North Australian and Kimberley Cratons during the 1835 to 1805 Ma Halls Creek Orogen (Blake et al., 1999).

2.2.3. Other prospective volcanic complexes

Volcanic systems analogous to those that host the Toongi and Brockman deposits include the Jurassic Garrowilla volcanics of New South Wales, and the extensive Cenozoic Central Volcano Province of Queensland and New South Wales (e.g., Jones et al., 2017). In some of these systems, fractional crystallisation of mafic magmas has produced trachytic to rhyolitic volcanic rocks with high rare metal contents. The ca. 29 Ma southern Peaks Ranges, central Queensland, have been identified as particularly prospective, with several large (~0.1 km^3) peralkaline rhyolite domes having consistent ore element concentration of ~0.6% ZrO_2 and ~ 0.15% TREO (Chandler and Spandler, 2020). Zirconium and REE are hosted by an agpaitic magmatic assemblage of dalyite and eudialyte group minerals as well as secondary alteration phases allanite, zirconium silicate, and REE fluorcarbonates. These igneous bodies intrude through the Bowen Basin in a location immediately above the boundary between the Thomson and New England Orogens. As with Toongi and Brockman, high metal contents were achieved via extensive fractionation of alkali mantle-derived magma, with hydrothermal alteration only responsible for localised REE redistribution within each volcanic complex (Chandler and Spandler, 2020).

2.3. Unconformity-related

An unusual ore style labelled unconformity-related REE mineralisation was defined by Nazari-Dehkordi et al. (2018, 2020), based on studies of the Browns Range heavy REE mineralisation, as outlined below. This mineralisation type is of particular economic interest due to their elevated contents of highly sought-after metals Dy and Tb. The ore style is made distinct by its simple ore mineralogy dominated by xenotime, and a structurally-controlled, sediment host ore setting with no genetic link to magmatism. While most economically-significant mineralisation of this type is currently recognised from north-western Australia, this REE mineralisation style has been identified in the Athabasca Basin Canada (Rabiei et al., 2017), and in phosphate-rich Cambrian sedimentary sequences that unconformably overlie the Mount Isa Inlier (e.g., Korella; Jaireth et al., 2014).

2.3.1. Browns Range

The western portion of the Browns Range Dome, northern Tanami Region (Fig. 3a), contains numerous heavy REE orebodies that lie close to, or on, a regional unconformity between Archean meta-arkose and meta-sandstones of the Browns Range Metamorphics and overlying Proterozoic Birrindudu Group sandstones (Nazari-Dehkordi et al. 2017, 2018, 2020). Most of the orebodies occur as stockworks of hydrothermal veins and breccias (up to 400 m in lateral extent and 10 m in width) within steeply-dipping faults and shear zones in the Browns Range Metamorphics. The ore minerals are xenotime and minor florencite, which both occur in several generations, together with quartz, hydrothermal white mica and hematite (Cook et al., 2013; Nazari-Dehkordi et al., 2020). Currently defined resources of 9.19 Mt. of ore grading at 0.66% TREO (Northern Minerals Ltd., 2019) are contained within the seven discrete orebodies, and it is likely that further resources will be defined in the near future.

In-situ U–Pb dating of ore xenotime from several deposits/prospects produced an age range for mineralisation of 1.65 to 1.60 Ga (Nazari-Dehkordi et al., 2020); this timeframe does not correspond to any known magmatism or orogeny in the region, and is appreciably younger than the ca. 1.72 Ga regional metamorphism (Fraser, 2002). Far field stresses produced by the distal Isan and Liebig Orogenies are invoked as drivers of large-scale fluid flow and faulting/shearing to accommodate ore formation in the region (Nazari-Dehkordi et al., 2018, 2020). Later stage(s) of xenotime recrystallisation between ca. 1.5 to 1.6 Ga may record distal effects of the Isan and Chewings Orogenies.

REE geochemistry and Sm–Nd isotope data provide clear evidence that the REE for mineralisation were leached from the Browns Range Metamorphics by saline fluids (Nazari-Dehkordi et al., 2018), while geochemical, fluid inclusion and stable isotope data (Nazari-Dehkordi et al., 2018, 2019, 2020; Nazari-Dehkordi and Spandler, 2019), all support an ore formation model that involves mixing between REE-bearing fluids from the Browns Range Metamorphics with phosphorus-bearing acidic fluid from the Birrindudu Group sandstones. Fluid mixing led to precipitation of REE phosphate minerals, and was most effective in fault zones on, or near, the regional unconformity.

2.3.2. John Galt

The John Galt prospect shares many similarities to the Browns Range mineralisation, except it is hosted within the 1.80 Ga Red Rock Basin of the Halls Creek Orogen (Fig. 3a; Tyler et al., 1995; Page et al., 2001). The Red Rock Basin largely comprises fine- to coarse-grained quartz-rich sandstones with interlayers of pebbly sandstone and conglomerate (Blake et al., 2000). As with Brockman and Cummins Range, John Galt is located close to the Hall Creek Fault, but perhaps of more significance is its proximity to the regional unconformity between the Red Rock Basin and overlying Paleoproterozoic Osmond Basin and Birrindudu Group sandstones (Hancock and Rutland, 1984).

REE mineralisation is exposed as networks of quartz-xenotime veins and breccias along major N-S trending faults and, most distinctively, along a ~ 100 m high ENE-trending escarpment. This structure extends for over 9 kms, with mineralisation recognised over a strike length of at least 1.2 kms and to a depth of at least 100 m. While a mineral resource is yet to be defined, assays of surface samples are particularly rich in heavy REE, with many returning very high TREO, in excess of 50% in some cases (Northern Minerals Ltd., 2019).

A mineralisation age for John Galt of 1.62 Ga was determined by U–Pb in xenotime by Morin-Ka et al. (2016), which is comparable to the timing of mineralisation at Browns Range, but again is significantly younger than any local magmatism or major orogenic event (Tyler et al., 2012). Ore genesis processes at John Galt are likely to be very similar to Browns Range given the parallels in geological setting and mineralisation style between the two areas.

2.4. Skarn and IOCG related

2.4.1. Mary Kathleen

High-temperature skarns have the potential to be an important global source of REE (Sahlström et al., 2019). This deposit group includes the Mary Kathleen U-REE deposit that is hosted within the Mary Kathleen Fold Belt of the Mount Isa Inlier, Queensland (Fig. 3b). The host rocks to mineralisation are a steeply-dipping sequence of calc-silicate rocks of the Corella Formation that experienced regional skarn metamorphism due to intrusion of the Burstal Granite at 1740 Ma, followed by deformation and amphibolite-facies regional metamorphism at ca. 1580 Ma (Oliver et al., 1999). Mineralisation at the Mary Kathleen deposit, and nearby Elaine Dorothy Cu + REE prospect (Fig. 3b), formed between 1550 and 1500 Ma (Oliver et al., 1999; Spandler et al., 2016), which postdates the regional skarn and deformation events.

The Mary Kathleen ore consists of high-grade uraninite + allanite ± garnet veins and vein networks that form ore shoots within the western limb of a tight regional syncline and alongside the N–S trending steeply-dipping Mary Kathleen shear zone (Oliver et al., 1999). Despite high REE grades (~4 wt% REE; Jaireth et al., 2014), the deposit is uneconomic for REE extraction due to challenges of mineral processing and radioactivity. Geochemical and Sm–Nd isotope data are consistent with local crustal source for the REE, rather than a mantle source (Oliver et al., 1999; Hammerli et al., 2014; Spandler et al., 2016), although A-type granitic magmatism of the regional 1540–1500 Ma Williams-Naraku Batholith (Wyborn, 1998) has been implicated as providing fluid, and/or heat for mineralisation (Spandler et al., 2016). Ore metals were mobilised by saline fluids, with ore mineral precipitation triggered by fluid mixing, or fluid unmixing/reaction, in an active regional shear system (Oliver et al., 1999; Hammerli et al., 2014).

2.4.2. Milo

Milo is a structurally controlled IOCG-style deposit with a REE-enriched halo that lies approximately 20 km east of the Mary Kathleen deposit in the Tommy Creek Domain of the Mount Isa Inlier (Fig. 3b). The deposit lies just north of the Highway Fault Zone, which represent a major bounding structure between the Tommy Creek Domain and the Mitakoodi Culmination (O'Dea et al., 2006). The inferred REE resource at Milo stands at 187 Mt. at 0.06% TREO (GBM Resources Limited, 2019). The deposit is hosted in a highly altered and structurally disrupted metasedimentary package, with calc-silicate rocks containing the bulk of the mineralisation (Harvey, 2014), although mineralisation is currently open to the north, south, and at depth.

Research work on Milo is limited to the honours thesis of Harvey (2014), who documented two main ore types; an early REE mineralisation, and an overprinting breccia style pyrite + pyrrhotite + chalcopyrite + magnetite (± Au ± Co) IOCG mineralisation. Gold occurs as the electrum inclusions in pyrite. Dark red apatite is the primary REE ore mineral, although allanite, REE-rich titanite, and REE-carbonates have also been documented. The REE ore occurs as discontinuous apatite-rich pods and zones within calc-silicate rock (Fig. 8a). The apatite is complexly zoned with primary Cl-REE-rich apatite partially replaced and overgrown by an assemblage of allanite plus F-bearing, REE-poor apatite (Harvey, 2014). In situ Sm-Nd isotope analysis of this latter assemblage by laser ablation multi-collector ICP-MS (see Spandler et al., 2016, for analytical details) provides an isochron age of 1544 ± 41 Ma (Fig. 8), which represents a minimum age for primary REE mineralisation. A maximum age for mineralisation is constrained to ca. 1600 Ma based on preliminary dating of pre ore metamorphic titanite (Harvey, 2014).

The Nd isotope composition of the ore (Fig. 8) together with the Cl-rich nature of the primary REE ore assemblage (Harvey, 2014) support an ore genesis model involving dissolution and transport of REE from crustal sources via advection of Cl-rich fluids, followed by REE ore deposition in structural traps in calc-silicate rocks. Development of the subsequent IOCG–style mineralisation was likely controlled by redox/desulfidisation reactions during fluid ingress along the contacts between calc-silicate and black slate units (Harvey, 2014). In general, this ore genesis model is comparable to those proposed for the Mary Kathleen and Elaine-Dorothy systems (Oliver et al., 1999; Spandler et al., 2016), and may be applicable to REE mineralisation across the Mount Isa region.

2.4.3. Olympic Dam

The supergiant Olympic Dam IOCG deposit contains in excess of 10.7 billion tonnes of Cu–U–Au–Ag ore (BHP, 2019), which also contains 0.3 wt% light REE (Schmandt et al., 2017). Major REE ore minerals are bastnäsite and florencite with subordinate synchysite, monazite and xenotime (Ehrig et al., 2012). Details of the geology and setting of the deposit are outlined in Ehrig et al. (2012), Skirrow et al. (2018) and Reid (2019). Although one of the largest concentrations of REE in the world (Fig. 1), extraction of REE is currently uneconomic due to the low grade, low heavy REE content, and fine grainsize of the

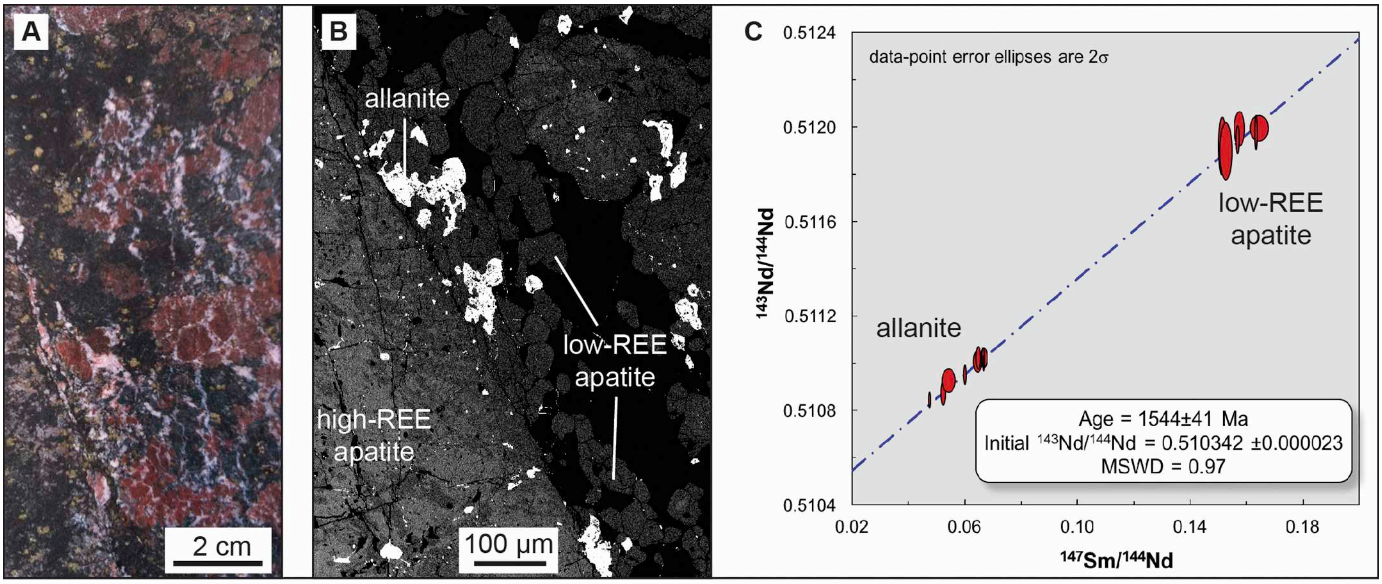

Fig. 8. REE ore from the Milo Deposit. (A) core photo of apatite (red) rich calc-silicate ore. (B) Backscattered electron (BSE) image of apatite rich ore with primary high-REE apatite (medium BSE intensity phase), and a secondary assemblage of low-REE apatite (low BSE intensity phase) and allanite (bright BSE). (C) Sm–Nd isochron of secondary REE-poor apatite and allanite ore assemblage. The age of this mineral assemblage provides a minimum age for primary mineralisation at Milo. (For interpretation of the references to colour in this figure legend, the reader is referred to the web version of this article.)

ore minerals. As with other ore metals, the REE mineralisation is associated with an extensive hematite-sericite-chlorite alteration assemblage within the Olympic Dam Breccia Complex, which itself is largely within the Roxby Downs Granite (Ehrig et al., 2012; Reid, 2019).

Olympic Dam lies in a major lithospheric boundary zone along the eastern margin of the Gawler Craton of South Australia. Geophysical surveys reveal that the deposit overlies a zone of highly metasomatised lithosphere that marks a major crustal scale fault zone that offsets the Moho (Heinson et al., 2018; Skirrow et al., 2018). The deposit was formed at ca. 1590 Ma and is interpreted to be coeval with emplacement of the extensive A-type Gawler Range Volcanics and Hiltaba Granite suites. An intracontinental extension setting is widely inferred for the region at this time, with various authors invoking various drivers of metamorphism and magmatism including a mantle plume (Betts et al., 2007) or lithospheric delamination (Skirrow et al., 2018). Mineralisation is thought to result from large scale mixing of deep lithospheric- or mantle-derived oxidised fluids, or igneous-derived fluids, with upper crustal (meteoric?) fluids (Heinson et al., 2018; Skirrow et al., 2018; Reid, 2019).

Geochronology of ore and alteration-related minerals reveal a protracted hydrothermal evolution for the deposit, with ages of 1400 to 1370 Ma, ca. 1100 Ma, 820 Ma, and 450–300 Ma (Huang et al., 2015; Cherry et al., 2018; Hall et al., 2018) obtained (Fig. 5). These ages are interpreted to reflect thermal perturbation or hydrothermal alteration related to regional orogenic or magmatic activity (Hall et al., 2018).

3. Discussion

3.1. Origin and formation of Australia's REE ore deposits

The complexity and diversity of REE ore deposits represents a challenge to understanding of how and where REE orebodies are formed. Nevertheless, a crucial advantage of studying these ore systems is that REE minerals tend to be excellent archives of geological events and conditions, as they sequester a large range of elements and isotopes that can be used to unravel geological histories and evolution. Combining mineral data with other geological information provides insights into the general processes and tectonic settings of ore formation. Consistent with the global situation (Weng et al., 2015), most of Australia's REE deposits are related to intraplate alkaline magmatism, including carbonatites, A-type granites, and peralkaline trachytes and rhyolites. By and large, these magmas are interpreted to be derivatives of primary magmas formed by low-degree melting of enriched mantle sources (e.g., Spandler and Morris, 2016; Marks and Markl, 2017). Extensive fractional crystallisation is considered to be crucial for magmatic enrichment of REE, as the enhanced solubility of REE in alkaline, fluorine-rich melts impedes early crystallisation of REE minerals and REE depletion from the evolving magma (Marks and Markl, 2017). Cumulate processes may nonetheless have been important for concentrating REE ore minerals in carbonatite-related deposits, such as Yangibana, Cummins Range and Nolans Bore (Anenburg and Mavrogenes, 2018; Slezak and Spandler, 2020).

In most of these magmatic deposits, hydrothermal alteration caused relatively minor and localised REE redistribution (e.g., Taylor et al., 1995b; Schoneveld et al., 2015; Spandler and Morris, 2016; Anenburg et al., 2018). Hydrothermal processes are, however, considered to be essential to ore formation in deposits where links to alkaline magmatism are equivocal (Mary Kathleen, Milo) or absent (Browns Range, John Galt). Defining the composition of hydrothermal fluids from ancient ore environments is always challenging, but for Browns Range and Mary Kathleen, the mineralising fluids are recognised to be high salinity brines sourced from underlying metasedimentary units (Oliver et al., 1999; Nazari-Dehkordi and Spandler, 2019). These fluid compositions are known to be effective REE transport agents (Williams-Jones et al., 2012).

All of the REE deposits described here are spatially associated with crustal-scale shear zones (e.g., Nolans Bore, Mary Kathleen) or boundaries between major crustal blocks (Yangibana, Mount Weld, Olympic Dam, Milo, Cummins Range, Brockman, Toongi, Peak Ranges) (see Table 1; Fig. 9). This association is unlikely to be coincidental; rather, these structures are regarded to be fundamental to ore formation, as they served as channelways to transport and focus metal-bearing fluids and/or melts from the deep crust and mantle to the site of ore formation.

3.2. Tectonic setting of Australia's REE ore deposits

Most of Australia's REE deposits are Mesoproterozoic in age and are

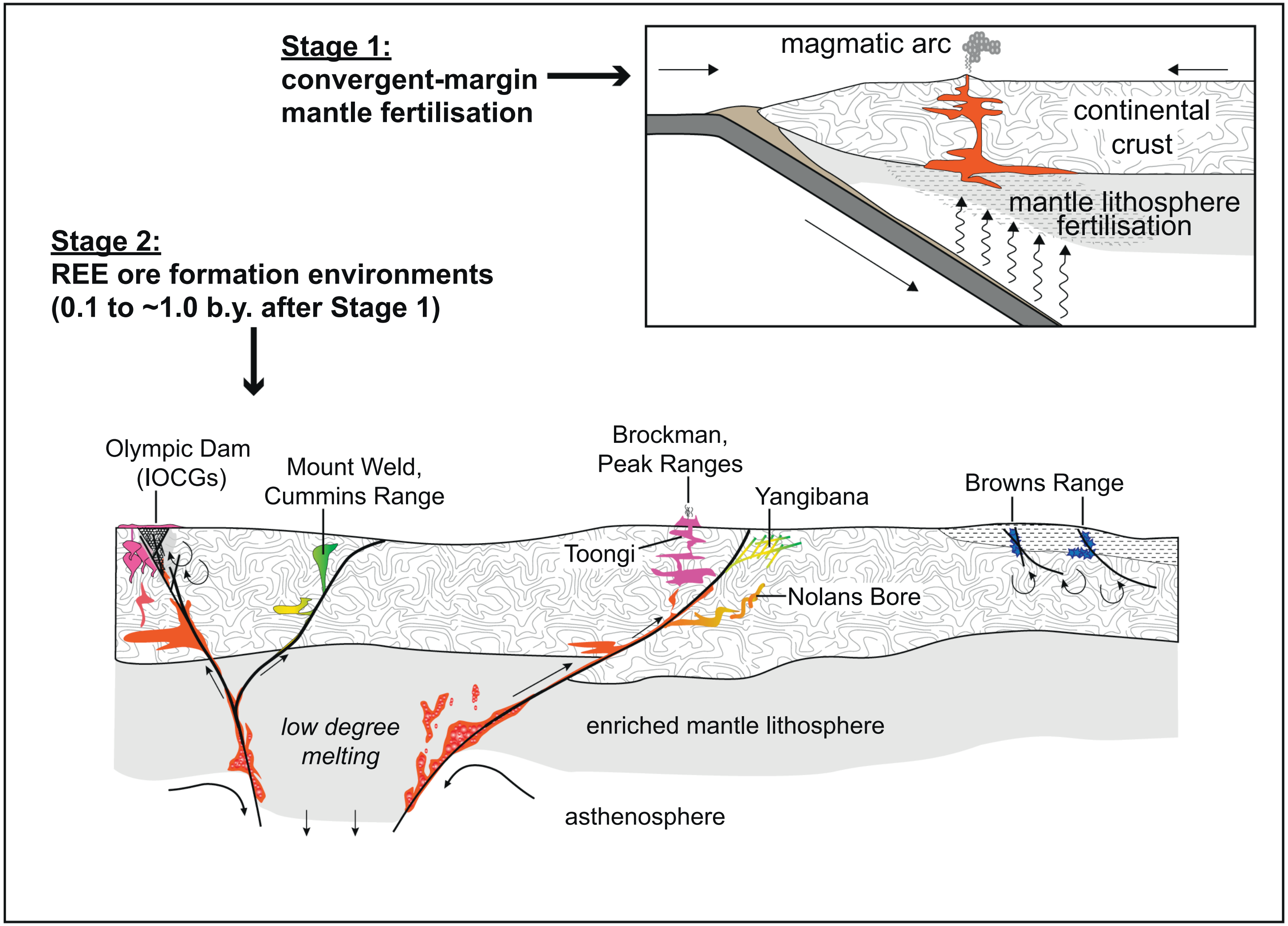

Fig. 9. Schematic cross section of continental lithosphere showing the formation environments of Australian REE deposits. Stage 1 (inset) depicts convergent margin activity leading to lithospheric mantle fertilisation. Stage 2 postdates Stage 1, and shows REE ore formation in an intracontinental setting under passive or extensional tectonic regimes. Low-degree melting of the previously-fertilised mantle lithosphere (particularly along lithosphere steps or lithospheric-scale structures) produces ore-productive magmas that ascend along crustal-scale fault zones to be emplaced in the mid to upper crust. Extensive fractional crystallisation or cumulate processing of these magmas is considered essential for reaching ore grade REE contents. Hydrothermal mobility and concentration of REE are critical for unconformity-related (Browns Range), IOCG and skarn deposits.

hosted in orogenic belts that have undergone extensive and repeated episodes of magmatism and orogenesis prior to REE mineralisation (see Table 1). The time gap between orogenic activity and REE ore formation ranges between ~100 and > 800 million years (Fig. 5). This prior history of orogenesis is considered to be crucial for mineralisation, as associated subduction-related metasomatism and magmatism led to the generation of subcontinental lithospheric mantle fertilisation (i.e., enrichment in incompatible elements and volatiles; see Fig. 9, stage 1). Subsequent melting of these enriched mantle domains is invoked to produce the distinctive alkaline magma compositions that are fertile for REE mineralisation (e.g., Marks and Markl, 2017). This premise is supported by radiogenic isotope signatures of the REE ores, including initial εNd values that largely fall in the range from −5 to +4 (Table 1; Fig. 6); these values are distinct from Mesoproterozoic to modern depleted mantle (εNd = +6 to +10), but are consistent with derivation from enriched mantle sources (Hawkesworth et al., 1984). Neodymium model ages for some ores also conform to episodes of prior orogenesis (e.g., Yangibana; Slezak and Spandler, 2020), although the geological significance of Nd model ages derived from REE-enriched materials is questionable.

The geodynamic setting responsible for producing REE ore-forming alkaline magmatism has been variably ascribed to mantle plumes (Pirajno, 2015), continental rift zones (Goodenough et al., 2016) and intracontinental fault activation due to far-field stresses (e.g., Downes et al., 2016; Slezak and Spandler, 2019). In many parts of the world spatial and temporal correlations exist between alkaline rock (e.g., carbonatites) and large igneous provinces (Ernst and Bell, 2010). However, for almost all of Australia's REE ore deposits, there is an absence of any spatial or temporal association with voluminous mafic magmatism (e.g., Huston et al., 2016; Downes et al., 2016; Spandler and Morris, 2016; Zi et al., 2017; Nazari-Dehkordi et al., 2018). Yangibana was linked to the ca. 1075 Ma Warakurna large igneous province by Pirajno et al. (2014), but is now well established to predate the Warakurna event by ca. 200 m.y. (Zi et al., 2017; Slezak and Spandler, 2019). Therefore, almost all of Australia's REE ore deposits do not conform to a mantle plume origin. The exceptions are Peak Ranges that formed as part of the Cosgrove hot spot track (Davies et al., 2015), and possibly the Mary Kathleen and Olympic Dam deposits, which have been suggested to have broad links to a mantle plume (Betts et al., 2007), although alternative geodynamic settings have also been proposed (e.g., delamination, Skirrow et al., 2018). In general, we do not consider hotspot-related magmatism to be particularly conducive for producing REE ores, as elevated mantle geotherms favour high-degree melting, which dilutes concentrations of incompatible elements such as REE in the melt. Nevertheless, deformation of the lithosphere distally to upwelling mantle plumes may be important for activation/reactivating lithospheric-scale structures to permit tapping of ore-fertile alkaline magmas from the mantle towards the surface (Ernst and Bell, 2010; Pirajno, 2015).

Of Australia's REE deposits, only the Brockman deposit is interpreted to have formed in a developing continental rift setting. While continental rifts are ideal for producing alkaline magmas that are fertile for REE mineralisation (e.g., Goodenough et al., 2016), active uplift and erosion, and structural dismemberment associated with these environments translates to a poor preservation potential for REE ores. This is especially true for Proterozoic mobile belts of Australia, which have experienced extensive and repeated periods of deformation and erosion.

Most of Australia's REE deposits are interpreted to have formed in intracontinental settings in isolation of active plate margins or mantle plumes (Fig. 9). The carbonatite-related ore deposits (Yangibana, Mount Weld, Cummins Range and, probably, Nolans Bore) likely developed during reactivation of lithospheric-scale fault zones due to far-field continental rifting or plate reorganisation. For example, formation of the Yangibana mineralisation is linked to distal effects of rifting of the North China and West Australian Cratons, which ultimately may also be linked to development of the Bayan Obo deposit at 1300 Ma (Fig. 4). A similar scenario is invoked for the Toongi deposit, which formed distally to the Karoo-Ferrar large igneous province along a major lithospheric boundary (Fig. 7). Such settings distal from active plate margins or voluminous magmatism may be especially conducive for the formation *and* preservation of REE ore deposits. Reactivation of lithospheric structures without anomalously high mantle geotherms (i.e., mantle plumes) or active asthenospheric upwelling (e.g., at plate margin environments) may provide ideal conditions for low-degree melting of enriched mantle lithosphere to produce incompatible-element enriched alkaline magmas; the most fertile magmas for REE mineralisation. Magma production may be triggered by decompression of enriched mantle lithosphere upthrown during fault movement, or heating of enriched lithosphere via juxtaposition with hot asthenosphere along a developing lithospheric step (e.g., King and Anderson, 1998; Skirrow et al., 2018). Fault reactivation also provides the conduits for transporting these fertile melts to the site of ore formation in the overlying crust (Fig. 9).

Unconformity-related deposits have no clear links to magmatism or mantle sources, but nonetheless also formed distal to active orogenesis and have a strong structural control on ore distribution (Nazari-Dehkordi et al., 2018; Nazari-Dehkordi et al., 2020). The broad tectonic setting of skarn and IOCG-related REE deposits remains highly debated (e.g., Reid, 2019), a situation further complicated when considering the essential role of local hydrothermal processes for mineralisation. Nevertheless, these deposits do have links to enriched mantle lithosphere and/or are controlled by large-scale intracontinental structures (e.g., Skirrow et al., 2018).

3.3. Post-mineralisation resetting events

Most REE ore deposits, being rich in phosphate and/or carbonate minerals, have contrasting rheology to their silicate host rocks. This, together with their close proximity to major crustal structures, means that REE ore deposits are susceptible to recystallisation or disturbance due to deformation events that may significantly postdate primary ore formation. As REE minerals have an affinity for Th and U, REE ores also retain radiogenic heat, which may further aid ore mineral recrystallisation. For example, Huston et al. (2016) calculated a radiogenic heat production of 270 μW/m^3 for the Nolans Bore deposit; a value more that 50 times the modern Australian crust value. This predisposition for REE mineral recystallisation presents a challenge for accurately dating primary ore formation, as radiogenic isotope systems commonly employed for this task (e.g., U–Pb or Sm–Nd) will also be reset or disturbed. We stress that interpretations of age dating results should be made in conjunction with careful textural evaluation and chemical analysis of mineral assemblages (e.g., Anenburg et al., 2018; Slezak et al., 2018). Without this detailed work, primary mineralisation ages may be incorrectly assigned much younger ages, as has been the case for Yangibana (see Pirajno et al., 2014; Zi et al., 2017; Slezak and Spandler, 2019), and the Bayan Obo deposit of Inner Mongolia (see Song et al., 2018).

Although these resetting events can complicate mineralisation age determinations, the geochronology and isotope geochemistry of REE ore minerals can also provide useful archives of regional tectonic or deformation events. This is well demonstrated by the mineral records of Nolans Bore, Yangibana, Cummins Range, Browns Range and Olympic Dam, all of which were subject to repeated ore mineral recystallisation during orogenic events that, in some cases, postdate the primary mineralisation by more than a billion years (Fig. 5, Table 1). For Nolans Bore and Yangibana, Nd isotope fingerprinting shows that these ore mineral recystallisation events were closed system; in other words, they were not accompanied by any additional external REE input, such as repeated alkaline magmatism (Fig. 6). Repeated reactivation of long-lived structures is recognised from continents across the globe (e.g., Will and Frimmel, 2018), but dating these events has long been a challenging endeavour. Using the geochronological archive of REE deposits can therefore compliment other thermochronometers applied to dating orogenic/structural events, such as Ar–Ar dating of micas. Australian deposits may be particularly useful in this regard, given their dominantly Precambrian age and their wide distribution across the country (Fig. 2).

3.4. Comparison to global REE deposits

In general, Australia's inventory of REE ore deposit types is similar to global record, with a majority related to carbonatites, peralkaline igneous rocks and IOCG systems (Weng et al., 2015; Van Gosen et al., 2017; Fig. 1). A notable difference is that Australia's peralkaline igneous-hosted deposits are volcanic in nature, whereas other deposits of this class around the world are related to intrusive rocks. The unconformity-related mineralisation style of Browns Range and John Galt is also not recognised globally, with the exception of the Maw Zone Deposit, Canada (Rabiei et al., 2017). However, this mineralisation style has only recently been defined (Nazari-Dehkordi et al., 2018), so we expect more occurrences of this type to be discovered across the globe in the future.

The generic model proposed here for many of Australia's REE deposits involves low degree melting of enriched sub-continental mantle lithosphere in an anorogenic setting, followed by extensive fractional crystallisation (with or without REE mineral accumulation). This model may apply to many other deposits across the globe, including Ilímaussaq, Greenland (Marks et al., 2004), the Strange Lake deposit, Canada (Siegel et al., 2017), the Mianning-Dechang REE belt, China (Hou et al., 2006; Liu and Hou, 2017), and the supergiant Bayan Obo deposit of Inner Mongolia, China (Smith et al., 2015), to name a few. It follows, therefore, that periods of relative quiescence in global tectonic activity may in fact be conducive for REE ore formation. We assess this premise by examining the age distribution of the world's REE ore deposits with reference to global tectonic conditions across Earth history.

Smith et al. (2016) showed that the world's largest REE deposits ($n = 15$) have age distribution peaks in the Mesoproterozoic and Phanerozoic. Our analysis of a much larger compilation of global REE deposits ($n = 139$) shows a similar age distribution (Fig. 10). The vast majority (~90%) are related to carbonatite and alkaline silicate magmatism. There is a notable dearth of deposits older than ~2.0 Ga, which we attribute to the lack of early convergent margin tectonics required to develop the enriched mantle sources that, in turn, are needed to produce ore-productive alkaline magmas. Many of the Phanerozoic deposits are associated with continental rift zones (e.g., Kola Peninsula; Goodenough et al., 2016), and are likely highly represented due to the relative abundance (Fig. 10) and favourable preservation conditions of these relatively young rocks.

The other major age clustering of REE deposits is from ca. 1.8 Ga to ca. 1.0 Ga (Fig. 10). Despite this time period accounting for only ~10% of the exposed continental crust (Goodwin, 1996), it accounts for around 35% of the world's—and most of Australia's—REE ore deposits (Fig. 10). This is all the more significant when considering that many of the world's largest REE resources, such as Bayan Obo, Ilímaussaq, and Mountain Pass, also formed within this timespan. This time period has previously been labelled the "boring billion" (Goldfarb et al., 2010; Roberts, 2013), due to a lack of environmental change or gold and base metal mineralisation forming during this time. On the other hand, the time window is recognised to be an important period for A-type magmatism, kimberlite emplacement and IOCG mineralisation (Goldfarb et al., 2010; Cawood and Hawkesworth, 2015). The period encompasses the transition from Nuna (or Columbia) to Rodinia, which was characterised by persistence of a stable supercontinent core, rather than extensive breakup and reassembly of a supercontinent mass (Roberts, 2013; Cawood and Hawkesworth, 2014). The relatively subdued geodynamic setting at this time may have been especially conducive for REE ore formation and preservation, for a number of reasons:

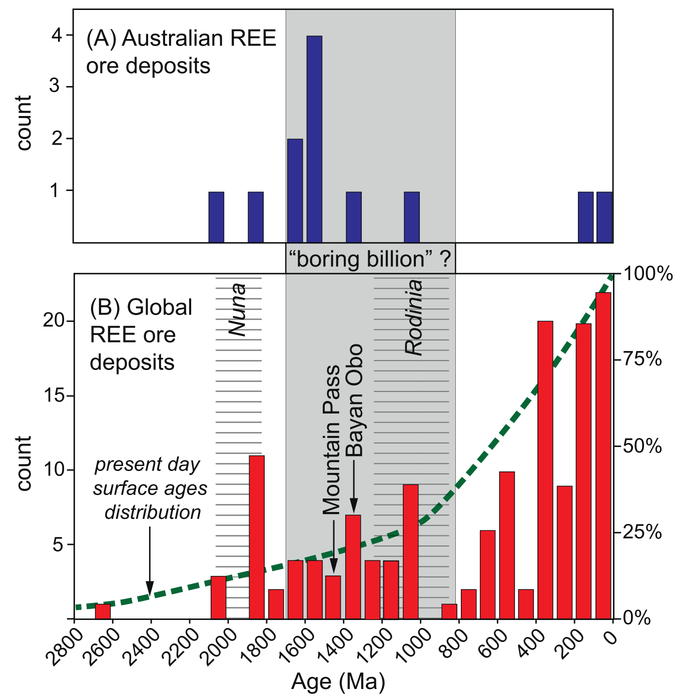

Fig. 10. Histograms of the age of; (A) Australian, and; (B) global REE ore deposits. The timing of amalgamation of the Nuna and Rodinia Supercontinents are shown in B, as well as the episode labelled the "boring billion" (Goldfarb et al., 2010). The present-day surface ages distribution curve (dashed green in panel B) is from Goodwin (1996), with percentage scale provided on the right side axis. Note the significant proportion of REE deposits in the Mesoproterozoic and Phanerozoic. A list of ore deposits with locations, ages and references are provided in Appendix 1. (For interpretation of the references to colour in this figure legend, the reader is referred to the web version of this article.)

1. Episodes of rifting of continental fragments and development of seafloor spreading leads to upwelling and high-degree melting of asthenosphere. Likewise, high-degree mantle melting is associated with convergent margin setting. Magmas produced in these setting are therefore not overtly fertile for REE mineralisation.
2. Previous episodes of plate convergence and supercontinent formation (e.g., Kenorland and Nuna supercontinent cycles) produced the enriched mantle sources that are required for generation of mineralisation-fertile magmas.
3. The mantle in the Mesoproterozoic was likely still sufficiently hot to allow low-degree partial melting with even slight physical or chemical perturbations, for example, by lithospheric deformation/faulting or volatile fluxing (e.g., Vaughan and Scarrow, 2003). By contrast, the overlying continental lithosphere was sufficiently cool and rigid (Cawood and Hawkesworth, 2014) to allow development of lithospheric-scale fault zones that could act as conduits for mineralisation-fertile magmas to ascend and evolve within the crust (Fig. 9).
4. Crustal preservation tends to be enhanced in stable continental interior, rather than in settings of continental rifting and/or amalgamation of continental fragments (Hawkesworth et al., 2009).

Far field stresses on the continental interior due to ongoing orogenic activity at the margins of the supercontinent, or distal plume events, are invoked as the drivers of lithospheric-scale fault activation, or reactivation (e.g., Jelsma et al., 2009), and associated low degree melting of the lithospheric mantle. In this sense, the REE ore productive magmas and mineralisation may be more easily produced through tectonic 'nudges' of continents, rather than extensive continental fragmentation or amalgamation. These conditions were well suited to the Mesoproterozoic or 'Earths middle ages' (Cawood and Hawkesworth, 2014), and may provide a rationale for the abundance of REE ore deposits, as well as kimberlites, IOCGs and A-type magmatism, formed at this time. The Mesoproterozoic is, therefore, far from 'boring'; rather, it can be seen as an important period of Earth's history linked with endowment in critical metals, such as REE, Zr, Nb, Ta, Cu and Co, that are of growing importance for sustaining modern society into the future.

4. Conclusions

- Australia hosts a diverse array of hard-rock REE ore deposits and is well placed to be a major REE producer into the future. Most deposits are related to alkaline igneous rocks, although hydrothermal processes were crucial to the formation of many deposits, most notably the unconformity-related REE deposits. REE enrichment via supergene alteration is also important for the economic viability of carbonatite-hosted REE deposits.
- Most deposits formed in an anorogenic setting in isolation of plate margins or mantle plumes. Ore–producing alkaline magmas were sourced from melting of enriched mantle sources, with extensive fractional crystallisation being a crucial process leading to ore formation. All deposits are closely associated with lithospheric-scale structures that likely act as conduits for transporting REE-bearing fluids and/or melts within the crust.
- A majority of Australia's deposits are Mesoproterozoic in age, although many preserve records of REE mineral recrystallisation due to orogenic or deformation events subsequent to ore formation. REE ore minerals can therefore be useful archives of geological events that affect continental interiors.
- The complex geology of most deposits, coupled with their remote locations, presents challenges for ore processing and economic viability, but also provides optimism that there may be many other REE orebodies within the Australian crust awaiting discovery.

Declaration of Competing Interest

The authors declare that they have no known competing financial interests or personal relationships that could have appeared to influence the work reported in this paper.

Acknowledgements

This study was made possible thanks to the generous assistance of Australian REE resource companies, Alkane Resources, Arafura Resources, GBM Resources, Hastings Technology Metals Ltd., and Northern Minerals Ltd. We also thank the staff at the Advanced Analytical Centre, JCU, for many years of supporting acquisition of geochemical/geochronological data on complex REE minerals. The manuscript has been greatly improved after reviews by Kathryn Goodenough and an anonymous reviewer. This research was supported by an Australian Research Council Future Fellowship (FT 120100198) to CS.

Appendix A. Supplementary data

Supplementary data to this article can be found online at https://doi.org/10.1016/j.earscirev.2020.103219.

References

Alkane Resources Limited (2015) Annual report 2015. http://www.alkane.com.au/index.php/reports/annual-reports.

Anenburg, M., Mavrogenes, J.A., 2018. Carbonatitic versus hydrothermal origin for fluorapatite REE-Th deposits: Experimental study of REE transport and crustal "antiskarn" metasomatism. Am. J. Sci. 318, 335–366.

Anenburg, M., Burnham, A.D., Mavrogenes, J.A., 2018. REE redistribution textures in altered fluorapatite: symplectites, veins, and phosphate-silicate-carbonate assemblages from the Nolans Bore P-REE-Th Deposit, Northern Territory, Australia. Can. Mineral. 56, 331–354.

Anenburg, M., Mavrogenes, J.A., Bennett, V.C., 2020. The fluorapatite P–REE–Th vein deposit at Nolans Bore: genesis by carbonatite metasomatism. J. Petrol. https://doi.org/10.1093/petrology/egaa003.

Betts, P.G., Giles, D., Schaefer, B.F., Mark, G., 2007. 1600-1500 Ma hotspot track in eastern Australia: Implications for Mesoproterozoic continental reconstructions. Terra Nova 19, 496–501.

BHP, 2019. Annual Report 2019. https://www.bhp.com/-/media/documents/investors/annual-reports/2019/bhpannualreport2019.pdf?la = en.

Blake, D.H., Griffin, T.J., Tyler, I.M., Thorne, A.M., Warren, R.G., 1999. Halls Creek First Edition (1:100,000 Scale Geological Map). Australian Geological Survey Organisation, Canberra.

Blake, D.H., Tyler, I.M., Page, R.W., 2000. Regional geology of the Halls Creek Orogen. In: Hoatson, D.M., Blake, D.H. (Eds.), Geology and Economic Potential of the Palaeoproterozoic Layered Mafic–Ultramafic Intrusions in the East Kimberley. Australian Geological Survey Organisation Bulletin 246, Western Australia, pp. 35–62.

Cawood, P.A., Hawkesworth, C.J., 2014. Earth's middle age. Geology 42, 503–506.

Cawood, P.A., Hawkesworth, C.J., 2015. Temporal relations between mineral deposits and global tectonic cycles. In: Jenkins, G.R.T., Lusty, P.A.J., McDonald, I., Smith, M.P., Boyce, A.J., Wilkinson, J.J. (Eds.), Geological Society of London Special Publication. 393. pp. 9–21.

Chandler, R., Spandler, C., 2020. The igneous petrogenesis and rare metal potential of the peralkaline volcanic complex of the southern Peak Range, Central Queensland, Australia. Lithos. https://doi.org/10.1016/j.lithos.2020.105386.

Cherry, A.R., Ehrig, K., Kamenetsky, V.S., McPhie, J., Crowley, J., Kamenetsky, M.B., 2018. Precise geochronological constraints on the origin, setting and incorporation of ca. 1.59 Ga surficial facies into the Olympic Dam Breccia complex, South Australia. Precambrian Res. 315, 162–178.

Conrad, C.P., Bianco, T.A., Smith, E.I., Wessel, P., 2011. Patterns of intraplate volcanism controlled by asthenospheric shear. Nat. Geosci. 4, 317–321.

Cook, N.J., Ciobanu, C.L., O'Rielly, D., Wilson, R., Das, K., Wade, B., 2013. Mineral chemistry of rare earth element (REE) mineralization, Browns Ranges, Western Australia. Lithos 172, 192–213.

Czarnota, K., Champion, D.C., Goscombe, B., Blewett, R.S., Cassidy, K.F., Henson, P.A., Groenewald, P.B., 2010. Geodynamics of the eastern Yilgarn Craton. Precambrian Res. 183, 175–202.

Davies, D.R., Rawlinson, N., 2014. On the origin of recent intraplate volcanism in Australia. Geology 42, 1031–1034.

Davies, D.R., Rawlinson, N., Iaffaldano, G., Campbell, I.H., 2015. Lithospheric controls on magma composition along Earth's longest continental hotspot track. Nature 525, 511–514.

Downes, P.J., Demény, A., Czuppon, G., Jaques, A.L., Verrall, M., et al., 2014. Stable H–C–O isotope and trace element geochemistry of the Cummins Range Carbonatite Complex, Kimberley region, Western Australia: implications for hydrothermal REE mineralization, carbonatite evolution and mantle source regions. Mineral. Deposita 49, 905–932.

Downes, P.J., Dunkley, D.J., Fletcher, I.R., et al., 2016. Zirconolite, zircon and monazite-(Ce) U-Th-Pb age constraints on the emplacement, deformation and alteration history of the Cummins Range Carbonatite Complex, Halls Creek Orogen, Kimberley region, Western Australia. Mineral. Petrol. 110, 199–222.

Ehrig, K., McPhie, J., Kamenetsky, V.S., 2012. In: Hedenquist, J.W., Harris, M., Camus, F. (Eds.), Geology and mineralogical zonation of the Olympic Dam iron oxide Cu-U-Au-Ag deposit, South Australia. Society of Economic Geologists Special Publication 16, pp. 237–268.

Ernst, R.E., Bell, K., 2010. Large igneous provinces (LIPs) and carbonatites. Mineral. Petrol. 98, 55-76.. 98, 55–76.

Fraser, G., 2002. Geochronology of Tanami ores and host rocks. In: Munson, T.J., Scrimgeour, I. (Eds.), Northern Territory Geological Survey Bulletin.

GBM Resources Limited (2019) Annual Report 2019. https://www.asx.com.au/asxpdf/20191024/pdf/449v1gf9qpb4hw.pdf.

Goldfarb, R.J., Bradley, D., Leach, D.L., 2010. Secular variation in economic geology. Econ. Geol. 105, 459–465.

Goodenough, K.M., Schilling, J., Jonsson, E., Kalvig, P., Charles, N., Tuduri, J., Deady, E.A., Sadeghi, M., Schiellerup, H., Müller, A., Bertrand, G., Arvanitidis, N., Eliopoulos, D.G., Shaw, R.A., Thrane, K., Keulen, N., 2016. Europe's rare earth element resource potential: an overview of REE metallogenetic provinces and their geodynamic setting. Ore Geol. Rev. 72, 838–856.

Goodwin, A.M., 1996. Principles of Precambrian Geology. Academic Press, London, pp. 327.

Graham, S., Lambert, D., Shee, S., 2004. The petrogenesis of carbonatite, melnoite and kimberlite from the Eastern Goldfields Province, Yilgarn Craton. Lithos (1–4), 519–533.

Hall, J.W., Glorie, S., Reid, A.J., Collins, A.S., Jurdan, F., Danišík, M., Evans, N., 2018. Thermal history of the northern Olympic Domain, Gawler Craton; correlations between thermochronometric data and mineralising systems. Gondwana Res. 56, 90–104.

Hammerli, J., Spandler, C., Oliver, N.H.S., Rusk, B., 2014. Cl/Br of scapolite as a fluid tracer in the earth's crust: insights into fluid sources in the Mary Kathleen Fold Belt, Mt. Isa Inlier, Australia. J. Metamorph. Geol. 32, 93–112.

Hancock, S.L., Rutland, R.W.R., 1984. Tectonics of an early Proterozoic geosuture: the Halls Creek orogenic sub province, northern Australia. J. Geodyn. 387–432.

Harvey, J., 2014. Geology and Genesis of the Milo REE + Y Deposit, Cloncurry District. James Cook University, Townsville, Australia, North Queensland BSc Hons. thesis.

Hastings Technology Metals Limited (2019) Annual Report 2019. https://hastingstechmetals.com/investor-relations/annual-reports/.

Hawkesworth, C.J., Rogers, N.W., Van Calsteren, P.W.C., Menzies, M.A., 1984. Mantle enrichment processes. Nature 311, 331–335.
Hawkesworth, C., Cawood, P., Kemp, T., Storey, C., Dhuime, B., 2009. A matter of preservation. Science 323, 49–50.
Heinson, G., Didana, Y., Soeffky, P., Thiel, S., Wise, T., 2018. The crustal geophysical signature of a world-class magmatic mineral system. Sci. Rep. 8, 10608.
Henson, P.A., Blewett, R.S., Roy, I.G., Miller, J.M., Czarnota, K., 2010. 4D architecture and tectonic evolution of the Laverton region, eastern Yilgarn Craton, Western Australia. Precambrian Res. 183, 338–355.
Hoatson, D., Jaireth, S., Miezitis, Y., 2011. The major rare-earth-element deposits of Australia: geological setting, exploration, and resources. Geoscience Australia 204.
Hou, Z., Tian, S., Yuan, Z., Xie, Y., Yin, S., Yi, L., et al., 2006. The Himalayan collision zone carbonatites in western Sichuan, SW China: petrogenesis, mantle source and tectonic implication. Earth Planet. Sci. Lett. 244, 234–250.
Huang, Q., Kamenetsky, V.S., McPhie, J., Ehrig, K., Meffre, S., Maas, R., Thompson, J., Kamenetsky, M., Chambefort, I., Apukhtina, O., Hu, Y., 2015. Neoproterozoic (ca. 820–830 Ma) mafic dykes at Olympic Dam, South Australia: Links with the Gairdner Large Igneous Province. Precambrian Res. 271, 160–172.
Huston, D.L., Maas, R., Cross, A., Hussey, K.J., Mernagh, T.P., Fraser, G., Champion, D.C., 2016. The Nolans Bore rare-earth element-phosphorus-uranium mineral system: geology, origin and post-depositional modifications. Mineral. Deposita 51, 797–822.
Jaireth, S., Hoatson, D.M., Miezitis, Y., 2014. Geological setting and resources of the major rare-earth-element deposits in Australia. Ore Geol. Rev. 62, 72–128.
Jelsma, H., Barnett, W., Richards, S., Lister, G., 2009. Tectonic setting of kimberlites. Lithos 112, 155–165.
Johnson, S.P., Thorne, A., Tyler, I., Korsch, R., Kennett, B., Cutten, H., et al., 2013. Crustal architecture of the Capricorn Orogen, Western Australia and associated metallogeny. Aust. J. Earth Sci. 60, 681–705.
Jones, I., Verdel, C., Crossingham, T., Vasconcelos, P., 2017. Animated reconstructions of the Late Cretaceous to Cenozoic northward migration of Australia, and implications for the generation of east Australian mafic magmatism. Geosphere 13, 460–481.
King, S.D., Anderson, D.L., 1998. Edge-driven convection. Earth Planet. Sci. Lett. 160, 289–296.
Kohanpour, F., Gorczyk, G., Lindsay, M.D., Occhipinti, S., 2017. Examining tectonic scenarios using geodynamic numerical modelling: Halls Creek Orogen, Australia. Gondwana Res. 46, 95–113.
Korsch, R.J., Totterdell, J.M., 2009. Subsidence history and basin phases of the Bowen, Gunnedah and Surat Basins, eastern Australia. Aust. J. Earth Sci. 56, 335–353.
Liu, Y., Hou, Z., 2017. A synthesis of mineralization styles with an integrated genetic model of carbonatite-syenite-hosted REE deposits in the Cenozoic Mianning-Dechang REE metallogenic belt, the eastern Tibetan Plateau, southwestern China. J. Asian Earth Sci. 137, 35–79.
Lottermoser, B.G., 1990. Rare-earth element mineralisation within the Mt. Weld carbonatite laterite, Western Australia. Lithos 24, 151–167.
Lynas Corporation Limited (2015) Annual Report 2015. https://www.lynascorp.com/wp-content/uploads/2019/05/151005-Annual-Report-1481137.pdf.
Marks, M.A.W., Markl, G., 2017. A global review on agpaitic rocks. Earth Sci. Rev. 173, 229–258.
Marks, M.A.W., Vennemann, T., Siebel, W., Markl, G., 2004. Nd-, O-, and H-isotopic evidence for complex, closed-system fluid evolution of the peralkaline Ilímaussaq intrusion, South Greenland. Geochim. Cosmochim. Acta 68, 3379–3395.
Meakin, N.S., Morgan, E.J. (1999) Dubbo 1:250 000 Geological Sheet SI/55-4, 2nd Edition. Geological Survey of New South Wales. Sydney, Explanatory Notes, 504.
Morin-Ka, S., Beardsmore, T.J., Hancock, E.A., Rasmussen, B., Dunkley, D., Muhling, J., Zi, J., Wilson, R., Champion, J., 2016. Alteration and Age of the Browns Range Rare Earth Element Deposits. Western Australian Department of Mines and Petroleum.
Mudd, G.M., Jowitt, S.M., 2016. Rare earth elements from heavy mineral sands: assessing the potential of a forgotten resource. Appl. Earth Sci. 125, 107–113.
Nazari-Dehkordi, T., Spandler, C., 2019. Paragenesis and composition of xenotime-(Y) and florencite-(Ce) from unconformity-related heavy rare earth element mineralization of northern Western Australia. Mineral. Petrol. 113, 563–581.
Nazari-Dehkordi, T., Spandler, C., Oliver, N.H.S., Chapman, J., Wilson, R., 2017. Provenance, tectonic setting and source of Archean metasedimentary rocks of the Browns Range Metamorphics, Tanami region, Western Australia. Australian J. Earth Sci. 64, 723–741.
Nazari-Dehkordi, T., Spandler, C., Oliver, N.H.S., Wilson, R., 2018. Unconformity-related rare earth element deposits: a regional-scale hydrothermal mineralization type of northern Australia. Econ. Geol. 113, 1297–1305.
Nazari-Dehkordi, T., Huizenga, J.M., Spandler, C., Oliver, N., 2019. Fluid inclusion and stable isotope constraints on the heavy rare earth element mineralisation in the Browns Range Dome, Tanami Region, Western Australia. Ore Geol. Rev. 113, 103068.
Nazari-Dehkordi, T., Spandler, C., Oliver, N.H.S., Wilson, R., 2020. Age, geological setting and paragenesis of heavy rare earth element mineralization of the Tanami Region, Western Australia. Mineral. Deposita 55, 107–130.
Nelson, D.R., Chivas, A.R., Chappell, B.W., McCulloch, M.T., 1988. Geochemical and isotopic systematics in carbonatites and implications for the evolution of ocean-island sources. Geochim. Cosmochim. Acta 52, 1–17.
Northern Minerals Limited (2019) 2019 Annual Report. https://northernminerals.investorportal.com.au/#announcements.
O'Dea, M.G., Betts, P.G., MacCready, T., Ailleres, L., 2006. Sequential development of a mid-crustal fold-thrust complex: evidence from the Mitakoodi Culmination in the eastern Mt. Isa Inlier, Australia. Aust. J. Earth Sci. 53, 69–90.
Olierook, H.K.H., Agangi, A., Plavsa, D., Reddy, S.M., Yao, W., Clark, C., Occhipinti, S.A., Kylander-Clark, A.R.C., 2019. Neoproterozoic hydrothermal activity in the West Australian Craton related to Rodinia assembly or breakup? Gondwana Res. 68, 1–12.
Oliver, N.H.S., Pearson, P.J., Holcombe, R.J., Ord, A., 1999. Mary Kathleen metamorphic-hydrothermal uranium-rare-earth element deposit: ore genesis and numerical model of coupled deformation and fluid flow. Aust. J. Earth Sci. 46, 467–484.
Page, R.W., Griffin, T.J., Tyler, I.M., Sheppard, S., 2001. Geochronological constraints on tectonic models for Australian Palaeoproterozoic high-K granites. J. Geol. Soc. Lond. 158, 535–545.
Pearson, J.M., Taylor, W.R., Barley, M.E., 1996. Geology of the alkaline Gifford Creek Complex, Gascoyne Complex, Western Australia. Aust. J. Earth Sci. 43, 299–309.
Pirajno, F., 2015. Intracontinental anorogenic alkaline magmatism and carbonatites, associated mineral systems and the mantle plume connection. Gondwana Res. 27, 1181–1216.
Pirajno, F., González-Álvarez, I., Chen, W., Kyser, K.T., Simonetti, A., Leduce, E., leGras, M., 2014. The Gifford Creek Ferrocarbonatite Complex, Gascoyne Province, Western Australia: Associated fenitic alteration and a putative link with the ~ 1075 Ma Warakurna LIP. Lithos 202-203, 100–119.
Pisarevsky, S.A., Wingate, M.T.D., Powell, C.McA., Johnson, S., Evans, D.A.D., 2003. Models of Rodinia assembly and fragmentation. In: Yoshida, M., Windley, B.F., Dasgupta, S. (Eds.), Proterozoic East Gondwana: Supercontinent Assembly and Breakup. 206. Geological Society of London Special Publications, pp. 35–55.
Rabiei, M., Chi, G., Normand, C., Davis, D.J., Fayek, M., Blamey, N.F.J., 2017. Hydrothermal rare earth element (xenotime) mineralization at Maw Zone, Athabasca Basin, Canada, and its relationship to unconformity-related uranium deposits. Econ. Geol. 112, 1483–1507.
Ramsden, A.R., French, D.H., Chalmers, D.I., 1993. Volcanic-hosted rare-metals deposit at Brockman, Western Australia. Mineral. Deposita 28, 1–12.
RareX Limited, 2020. Developing the Globally Significant Cummins Range Rare Earths Project. In: Investor presentation, . https://www.rarex.com.au/investor-presentation.
Reid, A., 2019. The Olympic Cu-Au Province, Gawler Craton: A Review of the Lithospheric Architecture, Geodynamic Setting, Alteration Systems, Cover Successions and Prospectively. Minerals 9, 371.
Roberts, N.M.W., 2013. The boring billion? - Lid tectonics, continental growth and environmental change associated with the Columbia supercontinent. Geosci. Front. 4, 681–691.
Sahlström, F., Jonsson, E., Högdahl, K., Troll, V.R., Harris, C., Jolis, E.M., Weis, F., 2019. Interaction between high-temperature magmatic fluids and limestone explains 'Bastnäs-type' REE deposits in Central Sweden. Sci. Rep. 9, 15203.
Schmandt, D.S., Cook, N.J., Ciobanu, C.L., Ehrig, K., Wade, B.P., Gilbert, S., Kamenetsky, V.S., 2017. Rare earth element fluorocarbonate minerals from the Olympic Dam Cu-U-Au-Ag deposit, South Australia. Minerals 7, 202.
Schmandt, D.S., Cook, N.J., Ciobanu, C.L., Ehrig, K., Wade, B.P., Gilbert, S., Kamenetsky, V.S., 2019. Rare earth element phosphate minerals from the Olympic Dam Cu-U-Au-Ag deposit, South Australia: recognizing temporal-spatial controls on REE mineralogy in an evolved IOCG system. Can. Mineral. 57, 3–24.
Schoneveld, L., Spandler, C., Hussey, K., 2015. Genesis of the central zone of the Nolans Bore rare earth element deposit, Northern Territory, Australia. Contrib. Mineral. Petrol. 170, 1–22.
Siegel, K., Williams-Jones, A.E., Stevenson, R., 2017. A Nd- and O-isotope study of the REE-rich peralkaline Strange Lake granite: implications for Mesoproterozoic A-type magmatism in the Core Zone (NE Canada). Contrib. Mineral. Petrol. 172, 54.
Skirrow, R.G., Van Der Wielen, S.E., Champion, D.C., Czarnota, K., Thiel, S., 2018. Lithospheric architecture and mantle metasomatism linked to iron oxide Cu-Au ore formation: Multidisciplinary evidence from the Olympic Dam Region, South Australia. Geochem. Geophys. Geosyst. 19, 2673–2705.
Slezak, P., 2019. Petrology of the Gifford Creek Carbonatite complex and the Yangibana LREE district, Western Australia: new insights from sotope geochemistry and geochronology. In: James Cook University, Townsville, Australia PhD Thesis.
Slezak, P., Spandler, C., 2019. Carbonatites as recorders of mantle-derived magmatism and subsequent tectonic events: an example of the Gifford Creek Carbonatite Complex, Western Australia. Lithos 328–329, 212–227.
Slezak, P., Spandler, C., 2020. Petrogenesis of the Gifford Creek Carbonatite Complex, Western Australia. Contrib. Mineral. Petrol. https://doi.org/10.1007/s00410-020-1666-3. (in press).
Slezak, P., Spandler, C., Blake, K., 2018. Ghosts of apatite past: using hyperspectral cathodoluminescence and micro-geochemical data to reveal multi-generational apatite in the Gifford Creek Carbonatite Complex, Australia. Can. Mineral. 56, 773–797.
Smith, M.P., Campbell, L.S., Kynicky, J., 2015. A review of the genesis of the world class Bayan Obo Fe–REE–Nb deposits, Inner Mongolia, China: multistage processes and outstanding questions. Ore Geol. Rev. 64, 459–476.
Smith, M.P., Moore, K., Kavecsánszki, D., Finch, A.A., Kynicky, J., Wall, F., 2016. From mantle to critical zone: a review of large and giant sized deposits of the rare earth elements. Geosci. Front. 7, 315–334.
Song, W., Xu, C., Smith, M.P., Chakhmouradian, A.R., Brenna, M., Kynicky, J., Chen, W., Yang, Y., Deng, M., Tang, H., 2018. Genesis of the world's largest rare earth element deposit, Bayan Obo, China: Protracted mineralization evolution over ~1 b.y. Geology 46, 323–326.
Spandler, C., Morris, C., 2016. Geology and genesis of the Toongi rare metal (Zr, Hf, Nb, Ta, Y and REE) deposit, NSW, Australia, and implications for rare metal mineralization in peralkaline igneous rocks. Contrib. Mineral. Petrol. 171, 104.
Spandler, C., Hammerli, J., Sha, P., Hilbert-Wolf, H., Hu, Y., Roberts, E., Schmitz, M., 2016. MKED1: a new titanite standard for in situ analysis of Sm–Nd isotopes and U–Pb geochronology. Chem. Geol. 425, 110–126.
Taylor, W.R., Page, R.W., Esslemont, G., Rock, N.M.S., Chalmers, D.I., 1995a. Geology of the volcanic-hosted Brockman rare-metals deposit, Halls Creek Mobile Zone, Northwest Australia. l. Volcanic environment, geochronology and petrography of the Brockman volcanics. Mineral. Petrol. 52, 209–230.

Taylor, W.R., Esslemont, G., Sun, S.-S., 1995b. Geology of the volcanic-hosted Brockman rare metals deposit, Halls Creek Mobile Zone, Northwest Australia. II. Geochemistry and petrogenesis of the Brockman volcanics. Mineral. Petrol. 52, 231–255.
Tyler, I.M., Griffin, T.J., Page, R.W., Shaw, R.D., 1995. Are there terranes within the Lamboo Complex of the Halls Creek Orogen? Geol. Survey Western Australia Ann. Rev. 1993 (94), 37–46.
Tyler, I.M., Hocking, R.M., Haines, P.W., 2012. Geological evolution of the Kimberley region of Western Australia. Episode 35, 298–306.
Van Gosen, B.S., Verplanck, P.L., Seal, R.R., II, Long, K.R., Gambogi, J. (2017) Rare-earth elements. In: Schulz, K.J., DeYoung, J.H., Jr., Seal, R.R., II, Bradley, D.C., eds. Critical mineral resources of the United States—Economic and environmental geology and prospects for future supply: U.S. Geological Survey Professional Paper 1802, O1–O31.
Vaughan, A.P., Scarrow, J.H., 2003. K-rich mantle metasomatism control of localization and initiation of lithospheric strike-slip faulting. Terra Nova 15, 163–169.
Veevers, J.J., 2012. Reconstructions before rifting and drifting reveal the geological connections between Antarctica and its conjugates in Gondwanaland. Earth-Sci. Rev. 111, 249–318.
Weng, Z.H., Jowitt, S.M., Mudd, G.M., Haque, N., 2013. Assessing rare earth element mineral deposit types and links to environmental impacts. Appl. Earth Sci. 122, 83–96.
Weng, Z., Jowitt, S.M., Mudd, G.M., Nawshad, H.A., 2015. A detailed assessment of global rare earth element resources: opportunities and challenges. Econ. Geol. 110, 1925–1952.
Will, T.M., Frimmel, H.E., 2018. Where does a continent prefer to break up? Some lessons from the South Atlantic margins. Gondwana Res. 53, 9–19.
Willett, G.C., Duncan, R.K., Rankin, R.A., 1986. Geology and economic evaluation of the Mt. Weld carbonatite, Laverton, Western Australia. In: Fourth international kimberlite conference, extended abstracts, pp. 97–99.
Williams-Jones, A.E., Migdisov, A.A., Samson, I.M., 2012. Hydrothermal mobilisation of the rare earth elements–a tale of “ceria” and “yttria”. Elements 8, 355–360.
Workman, R.K., Hart, S.R., Jackson, M., Regelous, M., Blusztajn, J., Kurz, M.D., Staudigel, H., 2004. Recycled metasomatized lithosphere as the origin of the Enriched Mantle II (EM2) end-member: Evidence from the Samoan Volcanic Chain. Geochem. Geophys. Geosyst. 5, Q04008.
Wyborn, L., 1998. Younger ca 1500 Ma granites of the Williams and Naraku Batholiths, Cloncurry district, eastern Mt Isa Inlier: geochemistry, origin, metallogenic significance and exploration indicators. Aust. J. Earth Sci. 45, 397–411.
Zhang, M., O'Reilly, S.Y., 1997. Multiple sources for basaltic rocks from Dubbo, eastern Australia: geochemical evidence for plume-lithospheric mantle interaction. Chem. Geol. 136, 33–54.
Zhang, S.-H., Zhao, Y., Li, X.-H., Ernst, R.E., Yang, Z.-Y., 2017. The 1.33-1.30 Ga Yanliao large igneous province in the North China Craton: Implications for reconstruction of the Nuna (Columbia) supercontinent, and specifically with the North Australian Craton. Earth Planet. Sci. Lett. 465, 112–125.
Zi, J.W., Gregory, C.J., Rasmussen, B., Sheppard, S., Muhling, J.R., 2017. Using monazite geochronology to test the plume model for carbonatites: the example of Gifford Creek Carbonatite Complex, Australia. Chem. Geol. 463, 50–60.